

Article

Brauer Analysis of Some Cayley and Nilpotent Graphs and Its Application in Quantum Entanglement Theory

Agustín Moreno Cañadas ^{1,*}, Ismael Gutierrez ^{2,*} and Odette M. Mendez ^{3,*}

¹ Departamento de Matemáticas, Universidad Nacional de Colombia, Edificio Yu Takeuchi 404, Kra 30 No. 45-03, Bogotá 11001000, Colombia

² Departamento de Matemáticas y Estadística, Universidad del Norte, Kilómetro 5, Vía Puerto Colombia, Barranquilla 081007, Colombia

³ Departamento de Matemáticas, Universidad Nacional de Colombia, Sede, La Nubia, Manizales 170003, Colombia

* Correspondence: amorenoca@unal.edu.co (A.M.C.); isgutier@uninorte.edu.co (I.G.); dmorenome@unal.edu.co (O.M.M.)

† These authors contributed equally to this work.

Abstract: Cayley and nilpotent graphs arise from the interaction between graph theory and algebra and are used to visualize the structures of some algebraic objects as groups and commutative rings. On the other hand, Green and Schroll introduced Brauer graph algebras and Brauer configuration algebras to investigate the algebras of tame and wild representation types. An appropriated system of multisets (called a Brauer configuration) induces these algebras via a suitable bounded quiver (or bounded directed graph), and the combinatorial properties of such multisets describe corresponding indecomposable projective modules, the dimensions of the algebras and their centers. Undirected graphs are examples of Brauer configuration messages, and the description of the related data for their induced Brauer configuration algebras is said to be the Brauer analysis of the graph. This paper gives closed formulas for the dimensions of Brauer configuration algebras (and their centers) induced by Cayley and nilpotent graphs defined by some finite groups and finite commutative rings. These procedures allow us to give examples of Hamiltonian digraph constructions based on Cayley graphs. As an application, some quantum entangled states (e.g., Greenberger–Horne–Zeilinger and Dicke states) are described and analyzed as suitable Brauer messages.

Keywords: Brauer configuration algebra; Cayley graph; nilpotent graph; path algebra; quantum entanglement; quiver representation



Citation: Cañadas, A.M.; Gutierrez, I.; Mendez, O.M. Brauer Analysis of Some Cayley and Nilpotent Graphs and Its Application in Quantum Entanglement Theory. *Symmetry* **2024**, *16*, 570. <https://doi.org/10.3390/sym16050570>

Academic Editor: Alice Miller

Received: 11 February 2024

Revised: 9 March 2024

Accepted: 13 March 2024

Published: 6 May 2024



Copyright: © 2024 by the authors. Licensee MDPI, Basel, Switzerland. This article is an open access article distributed under the terms and conditions of the Creative Commons Attribution (CC BY) license (<https://creativecommons.org/licenses/by/4.0/>).

1. Introduction

Cayley and nilpotent graphs are helpful combinatorial tools for the visualization of different algebraic structures [1–6]. On the one hand, Cayley graphs were introduced as a consequence of Cayley’s theorem; in such a case, given a group G and a subset $S \subseteq G$, the Cayley graph is an undirected graph $\mathcal{C}_{(G,S)} = (V_{\mathcal{C}_{(G,S)}}, E_{\mathcal{C}_{(G,S)}})$ whose set of vertices $V_{\mathcal{C}_{(G,S)}} = G$. Furthermore, there is an edge $e_{g_1, g_2} \in E_{\mathcal{C}_{(G,S)}}$ connecting two elements $g_1, g_2 \in G$ if there is an element $s \in S$ such that $g_1 s = g_2$ [1].

Investigations regarding Cayley graphs study graph properties such as connectedness, amenability, perfect matchings, algebraic degrees, chromatic and clique numbers or the existence of Hamiltonian paths [7–10]. The spectrum of the adjacency matrix of a Cayley graph allows interactions between graph, group representation and graph energy theories [11,12]. In particular, Sarmin et al. [12] studied the Seidel energy for Cayley graphs associated with dihedral groups. Moreover, Cayley graphs of groups and semigroups allow applications in cryptography via the construction of provably secure hash functions [13–16].

Currently, Cayley graphs are used to design good models of network architectures. The pancake and star graphs introduced by Akers and Krishnamurthy are examples of

Cayley graphs commonly accepted as models for such architectures. Butterfly networks are also examples of these kinds of graphs.

On the other hand, nilpotent graphs associated with rings have been studied by Chen, Khojasteh et al., Basnet et al. and Riyas et al. [5,6,17]. If R is a ring and $Nil(R) = \{x \in R \mid x^n = 0 \text{ for some positive integer } n\}$ is a ring R set of nilpotent elements, then the nilpotent graph $\mathcal{N}(R) = (V_{\mathcal{N}(R)}, E_{\mathcal{N}(R)})$ of the ring R has $R \setminus Nil(R)$ as a set of vertices. Two elements $x, y \in R, x \neq y$ are connected by an edge $e_{x,y} \in E_{\mathcal{N}(R)}$, if $x + y \in Nil(R)$. Studies dealing with nilpotent graphs are similar to those presented for Cayley graphs [6].

Green and Schroll [18,19] introduced Brauer configuration algebras to investigate algebras of the wild representation type. These algebras are bounded path algebras induced by a suitable collection of multisets Γ , i.e., such algebras are generated by paths in a directed graph or quiver Q_Γ whose vertices correspond to the multisets in Γ . In such a case, each element $x \in U \cap V$ with $U, V \in \Gamma$ defines an arrow $\alpha_{U,V}^x$ connecting U and V . Afterwards, Espinosa [20] introduced the Brauer message of a Brauer configuration. Such a definition allowed for the application of the theory of Brauer configuration algebras in different science and mathematics fields. Undirected graphs are mainly examples of Brauer messages. Therefore, Cayley and nilpotent graphs give rise to Brauer configuration algebras, whose associated multisets and the dimensions of their centers are defined by the number of corresponding edges.

Recently, Brauer configuration algebras have been a helpful tool for research on graph energy theory, block cyphers in cryptography, the Yang–Baxter equation and the number of zinc sulfide (ZnS) molecules in clusters of n layers in zinc-blended crystals [21–25].

This paper defines the Brauer configuration algebras induced by some finite groups and finite commutative rings via their associated Cayley and nilpotent graphs. It gives the dimensions of these algebras, the structures of their indecomposable projective modules, the dimensions of their centers and examples of Hamiltonian Brauer quivers. Furthermore, we describe new applications to the Brauer configuration algebra theory in quantum entanglement theory; specifically, we prove that quantum GHZ entanglement states of type GHZ_n^d and entanglement Dicke states of type D_n^m , recently realized in the laboratory, can be seen as suitable Brauer messages [26–30].

1.1. Motivations

Cayley and nilpotent graphs are undirected graphs that allow the visualization of algebraic structures as groups and rings. Research on these graphs establishes relationships between algebra and combinatorics. Since undirected graphs are Brauer messages, the Brauer analysis of the corresponding Brauer configuration algebras allows new interactions between representations of algebras, groups and graph theories.

If a given algebraic structure is associated with an undirected graph, it is suitable for a Brauer analysis. For instance, recently, Zeilinger et al. [28–30] realized experiments to derive the quantum entanglement states of type GHZ and D_n^m ; such entanglements give rise to appropriate undirected graphs whose perfect matchings allow their final states.

1.2. Contributions

The main contributions of this paper are Theorem 1, Proposition 2, Corollary 1, Theorem 2, Corollary 2, Theorems 3–5, Corollary 5, Theorems 6–8 and Corollary 6. This paper presents Brauer analyses of nilpotent and Cayley graphs associated with some groups and commutative rings. As an application, some GHZ and Dicke states are defined as appropriate Brauer messages.

Theorem 1 proves that the Brauer configuration algebra induced by a Cayley graph defined by a set of generators of a group G satisfies the length grading property (see the fifth item in Remark 2), and closed formulas for the dimensions of these algebras and their centers are also given. Proposition 2 gives similar results for the dimensions of Brauer configuration algebras induced by butterfly graphs. Corollary 1 establishes relationships between star and pancake graphs, which help to design network interconnections. Theorem 2

gives conditions for the construction of Hamiltonian Brauer quivers, and Corollary 2 gives an example of a Hamiltonian directed graph induced by a Cayley graph.

Theorems 3–5 are devoted to the properties of Brauer configuration algebras induced by nilpotent graphs. Theorem 3 proves that Brauer configuration algebras induced by nilpotent graphs $\mathcal{N}(\mathbb{Z}_{2^n})$ satisfy the length grading property, and the dimensions of these algebras and their centers can be obtained via some closed formulas. Theorems 4 and 5 give similar results for Brauer configuration algebras induced by nilpotent graphs of the form $\mathcal{N}(\mathbb{Z}_{2^{n_1 p_1 p_2 \dots p_t}})$ and $\mathcal{N}(\mathbb{Z}_{p_1^{a_1} p_2^{a_2} \dots p_t^{a_t}})$, where p_j denotes an odd prime number and a_i is a positive integer. Corollary 5 gives closed formulas for the centers of Brauer configuration algebras induced by connected components of some nilpotent graphs.

Theorems 6–8 and Corollary 6 give the main properties of the Brauer configuration algebras induced by quantum entanglements of type GHZ_n^2 , GHZ_n^3 , W_n and $D_n^{n/2}$. They also prove that the corresponding final states are specialized Brauer messages.

2. Preliminaries

This section gives basic definitions and notations regarding Cayley and nilpotent graphs associated with groups and commutative rings. It also introduces the notion of Brauer configuration algebra. Section 2.5 recalls the basic notations and definitions of quantum entanglement theory.

2.1. Background

The Cayley graph of a group was introduced in 1878 by Cayley [1]; since then, many works have been devoted to its properties and applications. According to Witte and Gallian [7], Rankin's paper [31] is the pioneering work regarding the existence of Hamiltonian cycles in Cayley digraphs.

Brian Alspach et al. [32] proved that every connected non-bipartite Cayley graph of valency at least three on a generalized dihedral group, whose order is divisible by four, is Hamilton-connected. Pastine and Jaume [33] proved that if S is a generating subset of a dihedral group D_n such that $D_n \cap S \neq \emptyset$, then the Cayley graph of D_n is Hamiltonian.

Riyas and Geetha [8] presented a study on the Cayley graphs over dihedral groups. They gave conditions for subgraphs of Cayley graphs associated with dihedral groups to be bipartite or Hamiltonian.

Applications of Cayley graphs in cryptography have been given by Charles and Lauter [14], Jao et al. [15] and Sosnovski [16], who used Cayley graphs associated with semigroups and groups to define provably secure hash functions.

Palanivel and Chithra [34] studied the energy and Laplacian energy of some Cayley graphs, whereas Sarmin et al. [12] investigated the Seidel energy for Cayley graphs associated with dihedral groups and Lu and Mönius [10] established the properties of the algebraic degree of Cayley graphs over abelian groups and dihedral groups.

The idea of using group theory to design interconnection networks was introduced in 1986 by Akers and Krishnamurthy, who presented some Cayley graphs named pancake and star graphs as examples of network architecture graphs. The butterfly and wrap-around butterfly networks are also examples of Cayley graphs in network design. The hypercube and the augmented cube are examples of the presence of Cayley graphs in networking research.

A vast body of literature is devoted to studying the properties of graphs defined by rings. Beck [2] introduced zero-divisor graphs to investigate the coloring problem in commutative rings. Afterwards, Anderson and Livingston [3] modified the notion of the zero-divisor graph introduced by Beck. Kala and Kavitha [4] also studied non-zero divisor graphs.

The notion of a weakly nilpotent graph of a commutative ring was introduced by Khojasteh and Nikmehr [5], and Basnet et al. [6] introduced nilpotent graphs for commutative rings whose edges connect non-nilpotent elements x, y with $x \neq y$ if $x + y$ is a nilpotent element. They gave conditions for rings of type \mathbb{Z}_n whose nilpotent graphs are connected, bipartite, regular or complete.

According to Schrödinger, quantum entanglement is the essence of quantum mechanics. Such a notion was introduced in 1935 by Einstein, Podolsky and Rosen to show the incompleteness of quantum mechanics theory. The trio, known as EPR, used perfect correlations of entangled states (called EPR states) to define so-called “elements of the reality”, which were missing in quantum theory, according to them [26].

EPR’s proposal was untestable for almost thirty years, until the introduction of Bell’s inequalities, which revealed that two-particle correlations for the two spin- $\frac{1}{2}$ singlet disagree with any local realistic model. Freedman and Clauser realized such an experiment in 1972, followed by Aspect et al. between 1981 and 1982. Meanwhile, the Greenberger–Horne–Zeilinger (GHZ) theorem showed that the concept of EPR’s elements is self-contradictory. We recall that the 2022 Nobel Prize was granted to Clauser, Aspect and Zeilinger for their experiments regarding quantum entanglement theory [27].

The interpretation of perfect matchings’ superposition as quantum entanglements was introduced by Gu, Zeilinger et al. [28–30]. They associated suitable undirected graphs with experimental quantum entanglements, so their perfect matchings allowed GHZ and Dicke entanglement states.

Green and Schroll [18,19] introduced Brauer graph algebras and Brauer configuration algebras. These algebras are generated by paths in a suitable quiver (digraph). Espinosa [20] introduced the message of a Brauer configuration, proving that any directed graph is the Brauer message of a Brauer configuration. This result proves that any algebraic structure whose elements and operations between them define an unoriented graph also induces a Brauer configuration algebra, and it is suitable for a Brauer analysis.

2.2. Graphs and Multisets

A graph \mathcal{G} is composed of two types of objects. It has a finite set $V_{\mathcal{G}} = \{a_1, a_2, a_3, \dots, a_n\}$ of elements called *vertices* and a set $E_{\mathcal{G}}$ of pairs of distinct vertices called *edges* [35]. We let $\mathcal{G} = (V_{\mathcal{G}}, E_{\mathcal{G}})$ denote a graph \mathcal{G} whose vertex set is $V_{\mathcal{G}}$, and whose edge set is $E_{\mathcal{G}}$, where $E_{\mathcal{G}} \subset V_{\mathcal{G}}^2$. A graph \mathcal{G} can be graphically represented by drawing a dot for each vertex and linking two of these dots with a line if they constitute an edge. It is considered irrelevant how these dots and lines are drawn. According to Diestel [36], all that matters is the information offered by the picture about the edges of the graph \mathcal{G} .

A quiver or digraph Q is a directed graph given by a system of the form (Q_0, Q_1, s, t) , where Q_0 (Q_1) is the set of *vertices* (*arrows*) of Q . s and t are maps $s, t : Q_1 \rightarrow Q_0$; $s(a)$ ($t(a)$) is said to be the *source* (*target*) of an arrow a . The graphical representation of a quiver Q is similar to the construction of a graph. In this case, two vertices (represented by dots) are connected by an arrow a whose starting vertex is the source $s(a)$ and the ending vertex is the target $t(a)$. A directed path is a sequence of arrows $P = \{a_0, a_1, \dots, a_{k-1}, a_k\}$ for which $s(a_i) = t(a_{i-1}), 1 \leq i \leq k$.

If Q is a digraph, $x \in Q_0$, $N_Q^-(x) = \{y \in Q_0 \mid (y, x) \in Q_1\}$, and $N_Q^+(x) = \{y \in Q_0 \mid (x, y) \in Q_1\}$, then the out-degree (in-degree) of x is denoted $d_Q^+ = |N_Q^+(x)|$ (denoted $d_Q^- = |N_Q^-(x)|$). The degree of a vertex x in Q is $d_Q(x) = d_Q^+(x) + d_Q^-(x)$ [37].

A *Hamilton cycle* of a graph G of order n is a cycle of G of length n . Hence, a Hamilton cycle in a graph of order n is a cycle $x_1 - x_2 - \dots - x_n - x_1$ of length n , where x_1, x_2, \dots, x_n are the n vertices of G in the same order. A *Hamilton path* in G joining vertices a and b is a path $a = x_1 - x_2 - \dots - x_n = b$ of length $n - 1$ of G . Thus, a Hamilton path is given by a permutation of the n vertices of G in which consecutive vertices are joined by an edge. The Hamilton path joins the first vertex of the permutation to the last. The edges of a Hamilton path and of a Hamilton cycle are necessarily distinct [35].

Let Q be a digraph for which $Q_0 = \{x_0, x_1, x_2, \dots, x_{n-1}, x_n\}$; then, a directed path P of the form $P = x_0 \rightarrow x_1 \rightarrow x_2 \rightarrow \dots \rightarrow x_{n-1} \rightarrow x_n$ is a Hamilton path of the digraph Q (each vertex appears just once in P). A digraph Q is Hamiltonian if it contains a Hamiltonian cycle. The decision problem of whether a graph has a Hamilton cycle is NP-complete [38]. This problem appears on Karp’s original list of 21 NP-complete problems.

Currently, there is a plethora of results regarding Hamiltonicity. For instance, Dirac proved that every graph on $n \geq 3$ vertices with minimum degree at least $n/2$ contains a Hamilton cycle. Meanwhile, Nash-Williams proved that if Q is a digraph on $n \geq 2$ vertices such that, for every vertex x , it holds that $d^+(x) \geq n/2$ and $d^-(x) \geq n/2$, then Q is Hamiltonian [39].

A multiset \mathfrak{M} is a pair $\mathfrak{M} = (M, f)$ of a set M and a map $f : M \rightarrow \mathbb{N}$, where \mathbb{N} is the set of nonnegative integers. f is said to be the *multiplicity function* associated with the set M . If $m \in M$, then $f(m)$ is the frequency of m in the multiset \mathfrak{M} , i.e., $f(m)$ denotes the number of times that m occurs in \mathfrak{M} . In this work, it is assumed that $f(m) \geq 1$ for any $m \in M$. In other words, a multiset is a set with possibly repeated elements [40].

Any finite multiset $\mathfrak{M} = (M, f)$ with $M = \{m_1, m_2, \dots, m_n\}$ can be written as a word $w(\mathfrak{M})$ with the form

$$w(\mathfrak{M}) = m_1^{f(m_1)} m_2^{f(m_2)} \dots m_n^{f(m_n)}. \quad (1)$$

A *permutation* of a multiset (1), $\pi \in S_{f(m_1)+f(m_2)+\dots+f(m_n)}$ is a word in which each letter belongs to M and, for each $m \in M$, the number of appearances of m in the word is $f(m)$ [40].

As an example, *symmetry* is a permutation of the multiset $e^1 m^2 r^1 s^1 t^1 y^2$. Such permutations give rise to labeled multisets of the form $(\mathfrak{M}, \pi) = \pi(w(\mathfrak{M}))$. According to Espinosa [20], a labeling (\mathfrak{M}, f) of a multiset \mathfrak{M} means that the word $w(\mathfrak{M})$ can be transformed using a suitable map $\varphi : M^* \rightarrow \mathfrak{A}$, where \mathfrak{A} is an appropriated set and M^* is the set of words induced by M . In such a case, it is assumed that (\mathfrak{M}, φ) is a multiset \mathfrak{M}' for which $w(\mathfrak{M}') = \varphi(w(\mathfrak{M}))$. Specifically, multiset permutations define labeled multisets.

If $\mathfrak{M}_1 = (M_1, f_1)$ and $\mathfrak{M}_2 = (M_2, f_2)$, then the interception $\mathfrak{M}_1 \cap \mathfrak{M}_2$ is defined in such a way that

$$\mathfrak{M}_1 \cap \mathfrak{M}_2 = \{m \in M_1 \cap M_2 \mid f(m) = \min\{f_1(m), f_2(m)\}\}. \quad (2)$$

According to Espinosa [20], the message $M(\mathcal{M})$ of a system of labeled multisets

$$\mathcal{M} = \{(\mathfrak{M}_1, \varphi_1), (\mathfrak{M}_2, \varphi_2), \dots, (\mathfrak{M}_n, \varphi_n) \mid \mathfrak{M}_j = (M_j, f_j), M = \bigcup_{j=1}^n M_j\} \quad (3)$$

with suitable maps φ_j , $1 \leq j \leq k$ is the concatenation of their words. That is,

$$M(\mathcal{M}) = w((\mathfrak{M}_1, \varphi_1))w((\mathfrak{M}_2, \varphi_2)) \dots w((\mathfrak{M}_n, \varphi_n)). \quad (4)$$

Graphs are examples of multiset messages. To see this, let $\mathcal{G} = (V_{\mathcal{G}}, E_{\mathcal{G}})$ be the graph for which $V_{\mathcal{G}} = \{0, 1, 2, 3\}$, $E_{\mathcal{G}} = \{e_i \mid 0 \leq i \leq 3\}$; the edges (multisets) are given by the following identities: $e_1 = \{1, 2\}$, $e_2 = \{2, 3\}$, $e_3 = \{3, 0\}$, $e_0 = \{0, 1\}$. The labeled edges are shown in Figure 1, where $a_i = i \pmod{4}$ ($b_i = i + 1 \pmod{4}$).

The graph shown in Figure 2 is the message $M(\mathcal{G})$ defined by the graph \mathcal{G} and the labeling $\{\varphi_i\}$, $0 \leq i \leq 3$.

Remark 1. Note that labeled messages of type (4) can be interpreted as elements of suitable algebraic objects. In fact, the first interpretation of such messages is as elements of a monoid determined by word-polygons. However, it is possible to enrich the structure $M(\mathcal{M})$ by adding a suitable collection of maps in such a way that $\varphi_i(w(\mathfrak{M}_i)) = \varphi_{i_i} \varphi_{i_{i-1}} \dots \varphi_{i_1}(w(\mathfrak{M}_i)) \in \mathfrak{A}$, for any $1 \leq i \leq n$, where \mathfrak{A} is an algebra endowed with a set of suitable operations $\mathcal{O}_{\mathfrak{A}} = \{\mathcal{O}_i \mid 1 \leq i \leq o_i\}$.

To obtain a specialized message $M^c(\mathcal{M})$ from $M(\mathcal{M})$, we consider that \mathfrak{A} is a Hilbert space of type \mathbb{C}^n , where \mathbb{C} denotes the complex numbers field and n is an appropriate integer number. Then, we define a partition $\mathcal{F} = \{F_1, F_2, \dots, F_p\}$ for the set of words induced by \mathcal{M} .

$$F_j = \{w(\mathfrak{M}_{j_i}) \mid 1 \leq t \leq t_j\}. \quad (5)$$

For j fixed and $O_{h_j} \in \mathcal{O}_{\mathfrak{A}}$, the specialized word $w^\epsilon(F_j)$ associated with F_j and $O_{h_j} \in \mathcal{O}_{\mathfrak{A}}$ is given by an identity of the form

$$w^\epsilon(F_j) = w(\mathfrak{M}_{j_1})O_{h_j}w(\mathfrak{M}_{j_2})O_{h_j} \dots O_{h_j}w(\mathfrak{M}_{j_{i_j-1}})O_{h_j}w(\mathfrak{M}_{j_{i_j}}) \in \mathfrak{B}. \tag{6}$$

where \mathfrak{B} is a suitable fixed Hilbert space. Often, $\mathfrak{B} = \mathfrak{A}$.

The specialized message $M^\epsilon(\mathcal{M})$ associated with the fixed operations $O_{h_1}, O_{h_2}, \dots, O_{h_p}, O_s \in \mathcal{O}_{\mathfrak{A}}$ is given by the following identity:

$$M^\epsilon(\mathcal{M}) = w^\epsilon(F_1)O_s w^\epsilon(F_2)O_s \dots O_s w^\epsilon(F_{p-1})O_s w^\epsilon(F_p) \in \mathfrak{B}. \tag{7}$$

A system of multisets as defined in (3) is said to be a Brauer configuration if it is endowed with a multiplicity function, $\mu : M \rightarrow \mathbb{N}^+$, and an orientation, \mathcal{O} , where \mathbb{N}^+ is the set of positive integers.



Figure 1. Edges are considered labeled multisets defined by a graph.

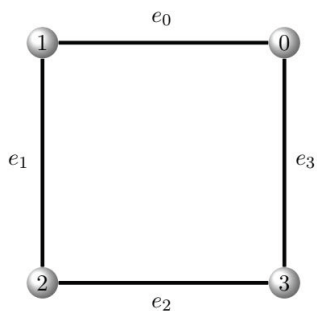


Figure 2. Example of a graph viewed as a message of a labeled system of multisets.

M^m denotes the intersection of all sets M_i that contain an element $m \in M$. $M^m = M_1^m \cap M_2^m \cap \dots \cap M_h^m$, $m \in M_s^m$, $M_s^m = M_i$ for some i , $1 \leq i \leq k$, $1 \leq s \leq h$. Then, we define a totally ordered set $(S_m, <)$ with $S_m = \{\mathfrak{M}_j^{m,n_j} \mid 1 \leq n_j \leq f_j(m), 1 \leq j \leq h\}$. Each element \mathfrak{M}_j^{m,n_j} corresponds to a copy of the multiset \mathfrak{M}_j .

The valency $val(m)$ of an element $m \in M$ (see (3)) is given by the sum.

$$val(m) = \sum_{j=1}^h f_j(m) \tag{8}$$

If $\mu(m)val(m) = 1$, then m is said to be truncated; otherwise, m is non-truncated. In this work, $\mu(m) = 2$ if $val(m) = 1$. Thus, the elements $m \in M$ in a Brauer configuration of type \mathcal{M} (also called vertices) are non-truncated. Multisets in Brauer configurations are named polygons by Green and Schroll [18].

The orientation \mathcal{O} is defined by extending the totally ordered set $(S_m, <)$ with a new relation of the form $\max S_m < \min S_m$. Thus, $C_m = (S_m, <) \cup \{\max S_m < \min S_m\}$ is a circular ordering associated with the point m .

A chain S_x is the successor sequence associated with the point x . Note that all the circular orderings defined by C_x are equivalent. Therefore, the Brauer configuration $(\mathcal{M}, \mu, \mathcal{O})$ defines a new multiset $\Gamma = (\{C_{m_i}\}, \delta_i)$ with $\delta_i(C_{m_i}) = \mu(m_i)$ and

$$w(\Gamma) = C_{m_1}^{\mu(m_1)} C_{m_2}^{\mu(m_2)} \dots C_{m_n}^{\mu(m_n)}, \quad M = \bigcup_{j=1}^k M_j = \{m_1, m_2, \dots, m_n\}. \quad (9)$$

As in the case for unoriented graphs, each circular ordering C_m is labeled with a digraph obtained by assigning to each covering of the form $\mathfrak{M}_h^{m, n_h} < \mathfrak{M}_j^{m, n_j}$ an arrow $\mathfrak{M}_h^{m, n_h} \xrightarrow{\alpha_{h,j}^m} \mathfrak{M}_j^{m, n_j}$. Such labeling associates each circular ordering with an oriented cycle called a *special cycle*. Therefore, the word $w(\Gamma)$ is nothing but a bounded quiver or digraph denoted Q_Γ , called the *Brauer quiver*, induced by the Brauer configuration Γ . For an algebraically closed field k , we let $\Lambda_\Gamma = kQ_\Gamma/I_\Gamma$ (in brief, $\Lambda = Q/I$) denote the bound quiver algebra generated by all the paths in Q bounded by an admissible ideal I_Γ generated by the following relations:

$$\begin{aligned} C_{m_i}^{\mu(m_i)} - C_{m_j}^{\mu(m_j)} & \text{ if } m_i, m_j \in \mathfrak{M}_s, \text{ for some } 1 \leq s \leq k \text{ (see 3)}. \\ C_{m_i}^{\mu(m_i)} f & \text{ if } f \text{ is the first arrow of } C_{m_i}. C_{m_i}^2 \in I_\Gamma, \text{ if } \text{val}(m_i) = 1. \\ \alpha_r^{m_i} \alpha_s^{m_j} & \text{ if } \alpha_r^{m_i} \alpha_s^{m_j} \in kQ_\Gamma, \alpha_r^{m_i} \in C_{m_i}, \alpha_s^{m_j} \in C_{m_j}, \text{ and } m_i \neq m_j. \end{aligned} \quad (10)$$

We recall [18] that a *multiserial algebra* is defined to be a finite dimensional algebra \mathcal{A} such that, for every indecomposable projective left and right \mathcal{A} -module P , the corresponding radical $\text{rad}(P)$ is a sum of uniserial modules (an \mathcal{A} -module M is said to be uniserial if it has a unique composition series), i.e., $\text{rad}(P) = \sum_{j=1}^m V_j$, where, for some integer m and uniserial modules V_j , it holds that if $i \neq j$, then $V_i \cap V_j$ is either 0 or a simple \mathcal{A} -module.

Remark 2. Green, Schroll and Sierra proved the following results regarding the structure of Brauer configuration algebras (see [18] Theorem B, Proposition 2.7, Theorem 3.10, Corollary 3.12 and [41] Theorem 4.9).

- There is a bijective correspondence between the set of indecomposable projective Λ -modules and the polygons in Γ .
- P is an indecomposable projective Λ -module corresponding to a polygon V in Γ . Then, $\text{rad } P$ is a sum of r indecomposable uniserial modules, where r is the number of (non-truncated) vertices of V and where the intersection of any two of the uniserial modules is a simple Λ -module.
- A Brauer configuration algebra is a multiserial algebra.
- The number of summands in the heart $\text{ht}(P) = \text{rad } P / \text{soc } P$ of an indecomposable projective Λ -module P such that $\text{rad}^2 P \neq 0$ equals the number of non-truncated vertices of the polygons in Γ corresponding to P counting repetitions.
- Let Λ be the Brauer configuration algebra associated with a connected Brauer configuration Γ . The algebra Λ has a length grading induced from the path algebra kQ if and only if there is an $N \in \mathbb{Z}_{>0}$ such that, for each non-truncated vertex, $\alpha \in \Gamma_0$ $\text{val}(\alpha)\mu(\alpha) = N$. In such a case, we say that the algebra Λ has the length grading property.
- The formula $\dim_k \Lambda = 2|M| + \sum_{m_i \in M} (\mu(m_i)\text{val}(m_i) - 1)$ gives the dimension of the Brauer configuration $\Lambda = kQ_\Gamma/I_\Gamma$ (see (3) and (8)).

- The dimension of the center $Z(\Lambda)$ of a connected and reduced Brauer configuration algebra Λ is given by the formula $\dim_k Z(\Lambda) = 1 + \sum_{m \in M} \mu(m) + |\mathcal{M}| - |M| + \#(\text{Loops } Q) - |\mathcal{C}_\Gamma|$, where $|\mathcal{C}_\Gamma| = \{\alpha \in \Gamma_0 \mid \text{val}(\alpha) = 1, \text{ and } \mu(\alpha) > 1\}$.

2.3. Cayley Graphs

If G is a group and $S \subseteq G$, then the Cayley graph $\mathcal{C}_{(G,S)}$ induced by the system (G, S) is an undirected graph whose set of vertices $V_{\mathcal{C}_{(G,S)}} = G$. In such a case, two elements $g_1, g_2 \in G$ are connected by an edge e , if there is an element $s \in S$ such that $g_1s = g_2$.

Cayley graphs are helpful tools in modeling interconnection networks. The vertices of the graph correspond to processing elements such as memory modules or switches, and the edges correspond to communication lines. For example, the Connection Machine has a network architecture that the 12-dimensional binary hypercube can model. Akers and Krishnamurthy introduced star and pancake graphs. They found that networks modeled by these types of graphs are superior to the binary n -cube when measured by degrees, diameter and connectivity. They found that networks based on star graphs possess the maximum connectivity and minimal degradation in the presence of faults [42].

The *butterfly* network and the cube-connected cycle network are vertex-symmetric graphs that are widely accepted as models for network architectures. An n -dimensional butterfly is a symmetric Cayley graph whose set of vertices $V = \{0, 1\}^n \times \{i \mid 0 \leq i \leq n\}$. Two vertices, (x, i) and (y, j) , are connected if and only if $j = i + 1$ and either $x = y$ or x and y only differ in the j th bit.

The following result gives the Cayley graph structure induced by group generator sets.

Proposition 1 ([42], Proposition 1.1). *Let S be a set of generators for a group G . The Cayley graph $\mathcal{C}_{(G,S)}$ has the following properties:*

1. $\mathcal{C}_{(G,S)}$ is a connected regular graph of degree equal to the cardinality of S ;
2. $\mathcal{C}_{(G,S)}$ is a vertex-symmetric graph.

Let n be a positive integer and $\mathbf{n} = \{1, 2, 3, \dots, n-1, n\}$. The n -dimensional *pancake graph* denoted by P_n is a graph (V_{P_n}, E_{P_n}) whose set of vertices $V_{P_n} = \{u_1u_2 \dots u_n \mid u_i \in \mathbf{n}, u_i \neq u_j \text{ if } i \neq j\}$. Two vertices $U = u_1u_2 \dots u_n$ and $V = v_1v_2 \dots v_n$ are connected by an edge $e \in E_{P_n}$ if $v_j = u_{i-j+1}$ for all $1 \leq j \leq i, 2 \leq i \leq n$. A sequence of the form $\{U_1, U_2, \dots, U_n\}$ denotes a sequence of vertices in P_n ; e denotes the vertex $123 \dots n$. A pancake graph P_n is an $(n-1)$ -regular graph with $n!$ vertices.

The *star graph* ST_n is defined to be the Cayley graph of the symmetric group \mathfrak{S}_n with respect to the generating set of transpositions $S = \{(1, 2), (1, 3), \dots, (1, n)\}$. Therefore, ST_n is a vertex transitive graph on $n!$ vertices with each vertex having degree $n-1$.

The *transposition graph* $\mathfrak{G}_\Delta = (V_{\mathfrak{G}_\Delta}, E_{\mathfrak{G}_\Delta})$ is a tool to represent graphically a set of transpositions $\Delta \subset \mathfrak{S}_n$. In such a case, $V_{\mathfrak{G}_\Delta} \subseteq \{1, 2, \dots, n\}$ and two vertices i and j are connected if the transposition $(i, j) \in \Delta$. Figure 3 shows the transposition graphs of the star graph ST_n and the pancake graph P_n .

As an example, Figures 4 and 5 show the way that the Cayley graph $\mathcal{C}_{(K,S)}$ ($K = \{e, a, b, ab \mid a^2 = b^2 = (ab)^2 = e\}$, $S = \{a, b\}$) induces a Brauer quiver $Q_{\mathcal{C}_{(K,S)}} = C_a C_{ab} C_b C_e$. In this case, $\mu(x) = 1$, for any $x \in K$. Oriented cycles $C_x = \alpha_1^x \alpha_2^x$ are attached to each $x \in K$.

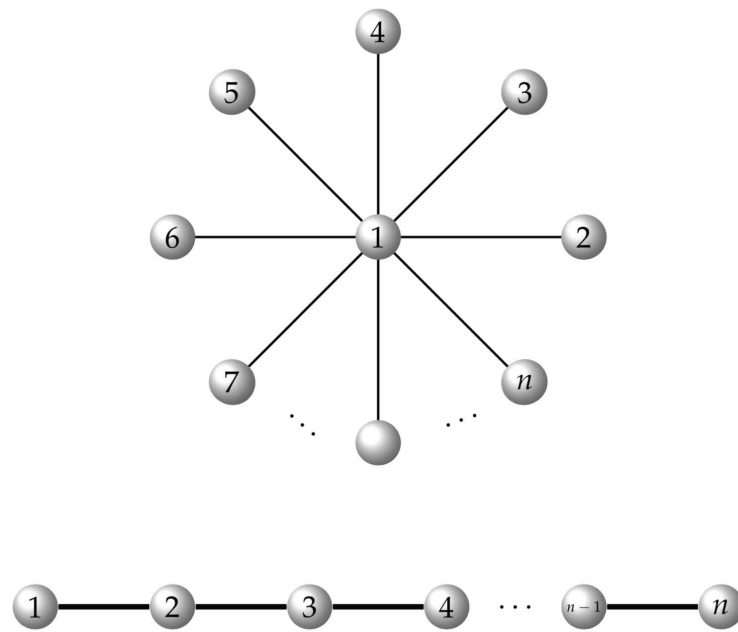


Figure 3. Transposition graphs of the star graph ST_n (above) and the pancake graph P_n (below).

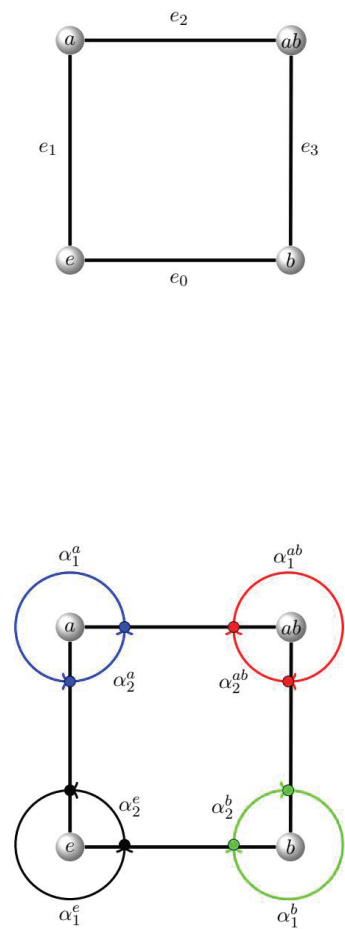


Figure 4. The Cayley graph of the Klein four-group and oriented cycles associated with its vertices.

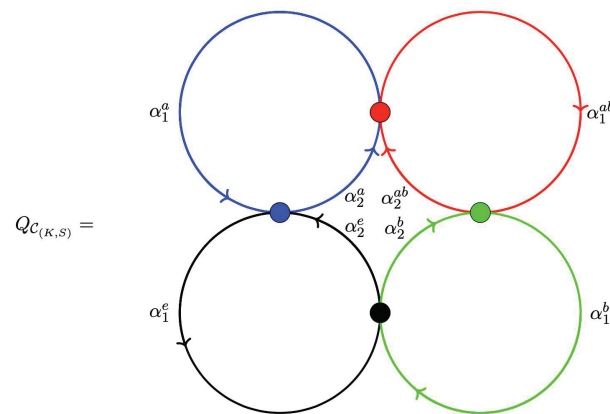


Figure 5. Construction of a Brauer quiver from the Cayley graph of the Cayley four-group. The oriented cycles associated with vertices in the same edge are identified.

Relations of the form (11) generate the ideal $I_{C_{(K,S)}}$ such that $\Lambda_{C_{K,S}} = kQ_{C_{(K,S)}}/I_{C_{(K,S)}}$ is a bound quiver algebra (Brauer configuration algebra). The same procedure can be applied to any graph \mathcal{G} for which the degree $deg(x) \geq 2$ for any vertex $x \in V_{\mathcal{G}}$.

$$\begin{aligned}
 &\alpha_1^x \alpha_2^x \alpha_1^x, \quad \alpha_2^x \alpha_1^x \alpha_2^x. \\
 &\alpha_1^a \alpha_2^a = \alpha_1^{ab} \alpha_2^{ab}, \quad \alpha_1^a \alpha_2^a = \alpha_1^e \alpha_2^e. \\
 &\alpha_1^b \alpha_2^b = \alpha_1^{ab} \alpha_2^{ab}, \quad \alpha_1^b \alpha_2^b = \alpha_1^e \alpha_2^e. \\
 &\alpha_i^x \alpha_j^x \alpha_i^x, \text{ for all possible values of } i, j \text{ and } x.
 \end{aligned}
 \tag{11}$$

2.4. Nilpotent Graphs

A nilpotent graph $\mathcal{N}(R)$ induced by a commutative ring (e.g., \mathbb{Z}_n) has $V_{\mathcal{N}(R)} = R \setminus Nil(R)$ as a set of vertices, where $Nil(R)$ denotes the set of nilpotent elements of R . Two elements $i, j \in V_{\mathcal{N}(R)}$ are connected by an edge $e \in E_{\mathcal{N}(R)}$ provided that $i + j \in Nil(R)$.

Nilpotent graphs associated with commutative rings have been studied by Chen, Khojasteh et al., Basnet et al. and Riyas et al. [5,6,17]. The following Remark 3 describes some properties of the nilpotent graphs associated with commutative rings of type \mathbb{Z}_n . These results are used to prove Theorems 3–5.

Remark 3. Basnet et al. (see [6], Lemma 2.1, Corollaries, 2.2, 2.4 and 2.5) proved that if a positive integer n can be written as a product of distinct odd prime numbers with the form $n = p_1^{a_1} p_2^{a_2} \dots p_t^{a_t}$, then the nilpotent graph $\mathcal{N}(\mathbb{Z}_n)$ induced by a commutative ring of type \mathbb{Z}_n is bipartite and consists of $\lfloor \frac{p_1 p_2 \dots p_t}{2} \rfloor$ disjoint complete bipartite subgraphs with $|Nil(\mathbb{Z}_n)|$ vertices of degree $|Nil(\mathbb{Z}_n)|$, denoted $K_{|Nil(\mathbb{Z}_n)|, |Nil(\mathbb{Z}_n)|}$. Furthermore, $\mathcal{N}(\mathbb{Z}_{2^s})$ is complete for $s \geq 1$.

Basnet et al. [6] also proved that if, in the product $n = p_1^{a_1} p_2^{a_2} \dots p_t^{a_t}$, $p_1 = 2$, and for $2 \leq j \leq t$, p_j is an odd prime, then the nilpotent graph $\mathcal{N}(\mathbb{Z}_n)$ consists of one complete subgraph of order $|Nil(\mathbb{Z}_n)|$ and its complement is bipartite, which is a union of disjoint complete bipartite subgraphs of type $K_{|Nil(\mathbb{Z}_n)|, |Nil(\mathbb{Z}_n)|}$. In particular, $deg(x) \in \{|Nil(\mathbb{Z}_n)|, |Nil(\mathbb{Z}_n)| - 1\}$ if $x \in V_{\mathcal{N}(\mathbb{Z}_n)}$.

Figure 6 shows the nilpotent graph $\mathcal{N}(\mathbb{Z}_8)$ whose set of vertices is $\mathbb{Z}_8 \setminus \{0, 2, 4, 6\} = \mathbb{Z}_8 \setminus Nil(\mathbb{Z}_8)$. The sums $1 + 7, 1 + 5, 1 + 3, 3 + 7, 3 + 5$ and $5 + 7$ define the edges $e_1 = \{1, 7\}$, $e_2 = \{1, 5\}$, $e_3 = \{1, 3\}$, $e_4 = \{3, 7\}$, $e_5 = \{3, 5\}$ and $e_6 = \{5, 7\}$, respectively.

It is easy to see that if $G = (\mathbb{Z}_{2^n}, +)$ is a 2^n -element additive group ($n \geq 1$) and $S = G \setminus \{0\}$, then the Cayley graph $C_{(G,S)}$ and the nilpotent graph $\mathcal{N}(\mathbb{Z}_{2^{n+1}})$ coincide as a consequence of Remark 3.

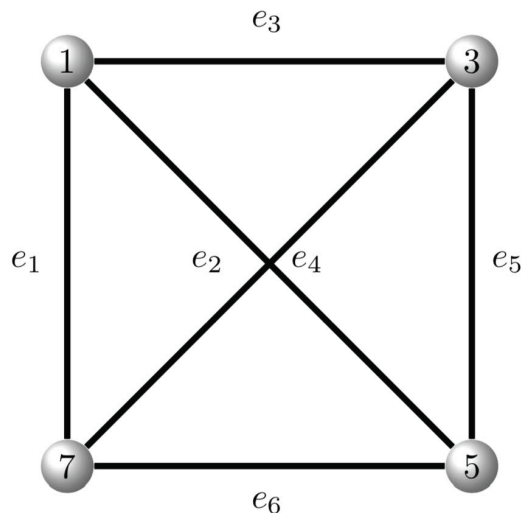


Figure 6. Nilpotent graph $\mathcal{N}(\mathbb{Z}_8)$ is a complete graph with four vertices and six edges.

2.5. Quantum Entanglement Theory

A qubit or quantum bit is a quantum system Ω whose state lies in a two-dimensional Hilbert space H .

A qubit is the most elementary unit of quantum information. It is a generalization of the notion of a bit in classical computing. A qubit can have two indistinguishable orthogonal states, denoted $|0\rangle$ and $|1\rangle$. In such a case, a qubit can be prepared as or transformed into any superposition of these two states, i.e.,

$$|\varphi_{qubit}\rangle = \alpha_0|0\rangle + \alpha_1|1\rangle, \quad \alpha_i \in \mathbb{C}, \quad \alpha_1^2 + \alpha_2^2 = 1. \tag{12}$$

A photon is an ideal candidate for a qubit.

$\Omega_1, \Omega_2, \dots, \Omega_n$ are quantum systems with underlying Hilbert spaces H_1, H_2, \dots, H_n , respectively. The global quantum system Ω is defined in such a way that its underlying Hilbert space \mathfrak{H} is given by the following identity:

$$\mathfrak{H} = \bigotimes_{i=1}^n H_i. \tag{13}$$

The following identities hold:

$$\begin{aligned} \begin{bmatrix} 1 \\ 0 \end{bmatrix} &= |0\rangle, \\ \begin{bmatrix} 0 \\ 1 \end{bmatrix} &= |1\rangle, \\ \begin{bmatrix} 1 \\ 0 \end{bmatrix} \otimes \begin{bmatrix} 1 \\ 0 \end{bmatrix} &= |0\rangle \otimes |0\rangle = |00\rangle = |0\rangle = \begin{bmatrix} 1 \\ 0 \\ 0 \\ 0 \end{bmatrix}, \\ \begin{bmatrix} 1 \\ 0 \end{bmatrix} \otimes \begin{bmatrix} 0 \\ 1 \end{bmatrix} &= |0\rangle \otimes |1\rangle = |01\rangle = |1\rangle = \begin{bmatrix} 0 \\ 1 \\ 0 \\ 0 \end{bmatrix}, \\ \begin{bmatrix} 0 \\ 1 \end{bmatrix} \otimes \begin{bmatrix} 1 \\ 0 \end{bmatrix} &= |1\rangle \otimes |0\rangle = |10\rangle = |2\rangle = \begin{bmatrix} 0 \\ 0 \\ 1 \\ 0 \end{bmatrix}, \\ \begin{bmatrix} 0 \\ 1 \end{bmatrix} \otimes \begin{bmatrix} 0 \\ 1 \end{bmatrix} &= |1\rangle \otimes |1\rangle = |11\rangle = |3\rangle = \begin{bmatrix} 0 \\ 0 \\ 0 \\ 1 \end{bmatrix}. \end{aligned} \tag{14}$$

Entanglement is a property of more than one quantum system such that the state of one system cannot be seen independently of the other's. It is the main source for many types of quantum information processing (e.g., quantum computing).

If $n = 2$, we assume that the quantum systems Ω_1 and Ω_2 have been separately prepared in states $|\varphi_1\rangle$ and $|\varphi_2\rangle$, and that they have been united without interacting. Thus, they lie in distinct Hilbert spaces H_1 and H_2 . In such a case, the physical predictions relating to one of these quantum systems do not depend in any way on the other quantum system.

The global quantum state Ω is called the *juxtaposition* of the quantum system Ω_1 and Ω_2 . The state of the global quantum system Ω is $|\varphi_1\rangle \otimes |\varphi_2\rangle$. If Ω_1 and Ω_2 are two qubits separately prepared in the states $\frac{1}{\sqrt{2}}(|0\rangle + |1\rangle)$ and $\frac{1}{\sqrt{2}}(|0\rangle + |1\rangle)$, then the state $|\varphi\rangle$ of the global system Ω is given by the following identity:

$$|\varphi\rangle = \frac{1}{2}(|00\rangle + |01\rangle + |10\rangle + |11\rangle). \quad (15)$$

Greenberger–Horne–Zeilinger (GHZ) and Dicke states D_n^k are classes of entangled states defined by the following identities:

$$\begin{aligned} |GHZ_n^d\rangle &= \frac{1}{\sqrt{d}} \sum_{i=0}^{d-1} |i\rangle^{\otimes n}. \\ |D_n^k\rangle &= \frac{1}{\sqrt{\binom{n}{k}}} \widehat{S}(|0\rangle^{\otimes(n-k)} |1\rangle^{\otimes k}). \end{aligned} \quad (16)$$

where n is the number of particles, k is the number of excitations, d is the dimension for every particle, and \widehat{S} is the symmetrical operator that gives summation over all distinct permutations of the n particles.

Zeilinger et al. [28–30] realized experimental setups based on *entanglement by path identity* to build $|GHZ_n^2\rangle$ and $|D_n^1\rangle = |W_n\rangle$ states. In the experiment, to create a $|GHZ_4^2\rangle$ state, four crystals were pumped coherently (crystals I and II had mode number $|00\rangle$, whereas crystals III and IV had mode number $|11\rangle$), and the pump power was set in such a way that pairs were produced with reasonable probabilities. They generalized the setup to find any $|GHZ_n^d\rangle$ state for $n > 1$ and $d = 2$.

The final quantum state was obtained by post-selection on four-fold coincidences, which meant that all four detectors clicked simultaneously. They associated with each of these experiments a suitable undirected graph $\mathcal{G}_{|\varphi\rangle}$ whose edges were labeled by appropriate quantum states (qubits). They calculated the tensor product of the labels attached to the perfect matchings of $\mathcal{G}_{|\varphi\rangle}$ and the sum of all these tensor products gave the state of the system ($|GHZ_n^2\rangle, |GHZ_4^3\rangle, |W_n\rangle, |D_n^{n/2}\rangle, |D_n^m\rangle, 0 < m < n$).

Figures 7 and 8 show a setup of type GHZ_4^2 , the induced undirected graph $\mathcal{G}_{|GHZ_4^2\rangle}$ (see [28–30]) and its perfect matchings giving the state $|GHZ_4^2\rangle = |0000\rangle + |1111\rangle$. Meanwhile, Figures 9 and 10 show a setup of type W_4 and its induced graph $\mathcal{G}_{|W_4\rangle}$, $|W_4\rangle = |0001\rangle + |0010\rangle + |0100\rangle + |1000\rangle$. The general $|W_n\rangle$ state gives rise to the so-called *Oliver_n* = $\mathcal{G}_{|W_n\rangle}$ graph [30].

In the last few years, quantum entanglement and quantum computing have paved the way for cryptography research. Nowadays, asymmetric cryptographic algorithms, used in key exchange protocols, appear to be most vulnerable to compromise by known quantum algorithms, specifically by Shor's algorithm. For instance, 2300 logical qubits are required to break the cryptographic system RSA based on the factoring problem. Given this potential threat to cybersecurity, the National Institute of Standards (NIST) began a process in 2016 to select and standardize replacement asymmetric cryptographic algorithms that are quantum-secure. The process was completed in 2022, when it was announced that CRYSTALS-KYBER and CRYSTALS-Dilithium were the new standards for post-quantum cryptography.

Jacques et al. implemented Grover oracles for the quantum key search on the Advanced Encryption Standard (AES). Grover's search algorithm gives a quantum attack

against block cyphers. Furthermore, Yin et al. developed, in a laboratory, a quantum key distribution (QKD) method to share secret keys based on quantum entanglement [43–45].

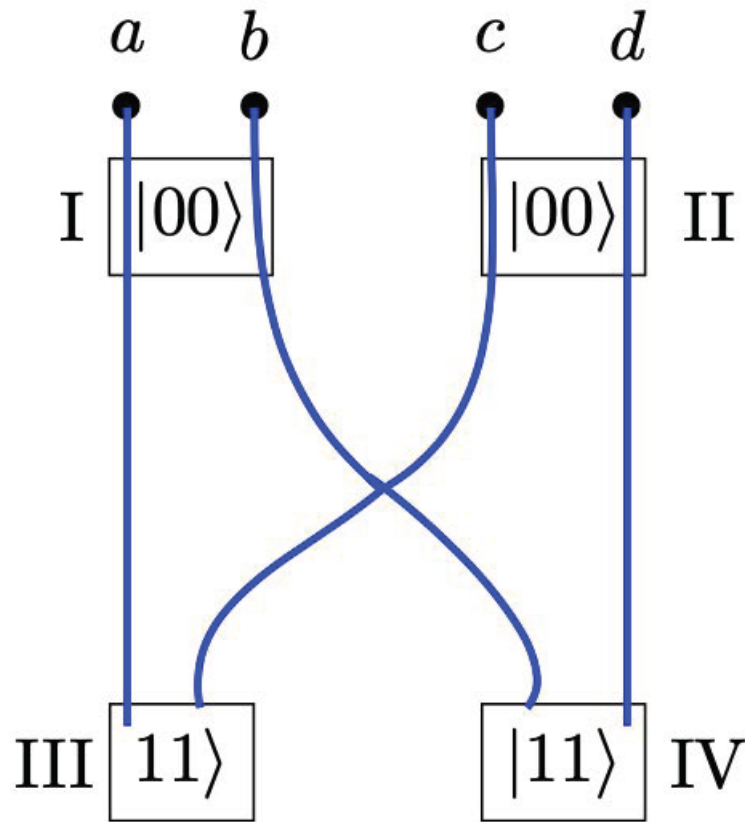


Figure 7. Setup of type GHZ_4^2 with four crystals and four particles.

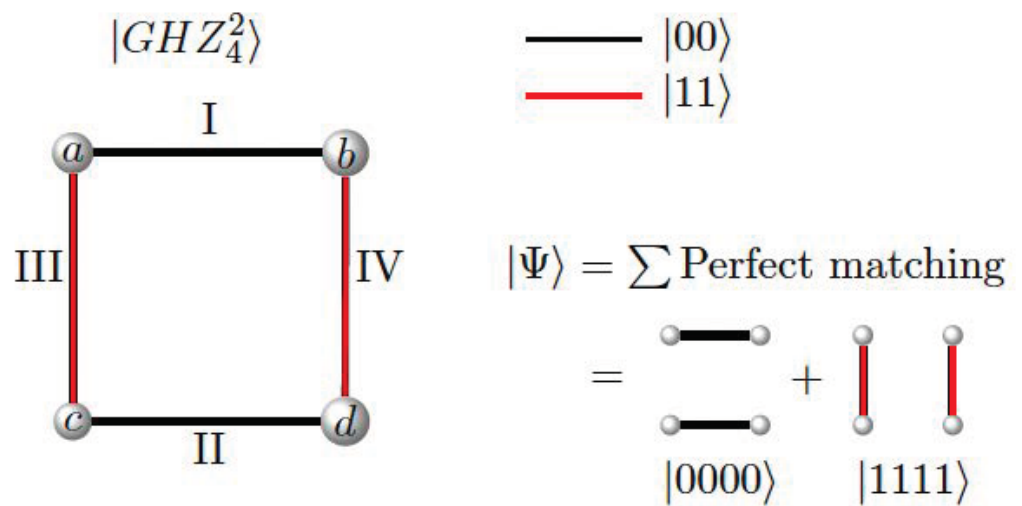


Figure 8. Graph $S_{|GHZ_4^2>}$ induced by a setup of type GHZ_4^2 (see Figure 7) and the perfect matchings giving $|GHZ_4^2>$.

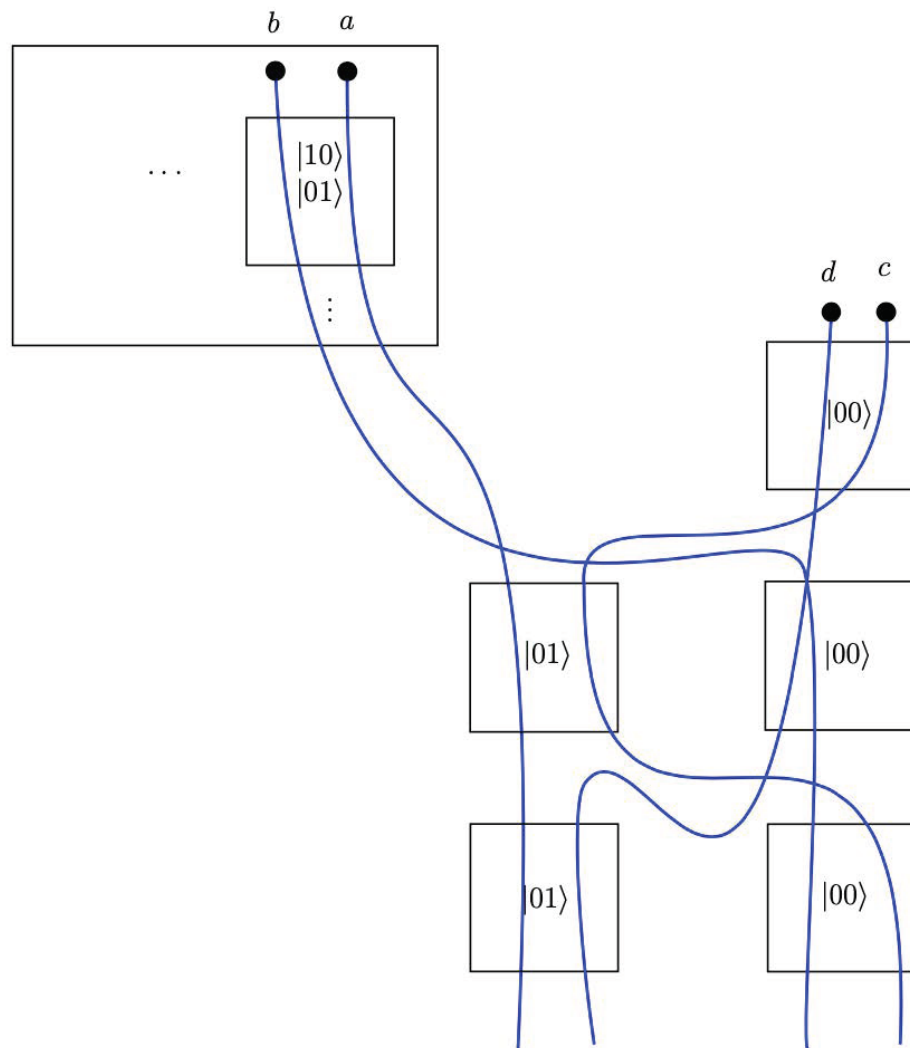


Figure 9. Setup of type W_4 with six crystals producing states $|00\rangle$, $|10\rangle$ and $|01\rangle$.

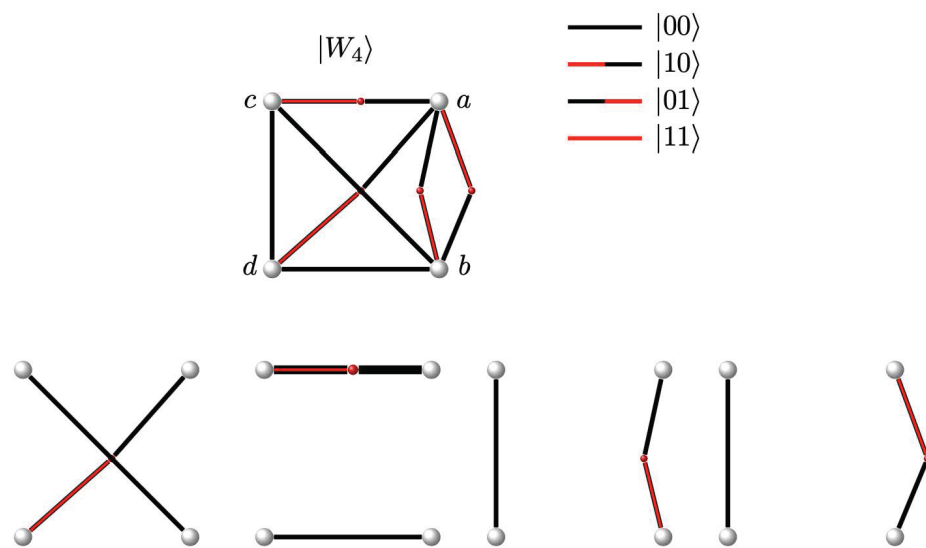


Figure 10. Graph $\mathcal{G}_{|W_4\rangle} = Oliver_4$ induced by a setup of type W_4 (see Figure 9). Its perfect matchings give the state $|W_4\rangle$.

3. Main Results

This section gives the main characteristics of the Brauer configuration algebras associated with Cayley graphs, star graphs, pancake graphs, butterfly graphs and some nilpotent graphs. Section 3.3 is devoted to the study of the Brauer configuration algebras induced by sets of type GHZ_n^d , W_n and D_n^m , $d \in \{2, 3\}$, $m = n/2$, $n \geq 4$.

3.1. Brauer Configuration Algebras Induced by Cayley Graphs

The following result provides the algebraic properties of the Brauer configuration algebras induced by some Cayley graphs.

Theorem 1. *The Brauer configuration algebra $\Lambda_{\mathcal{C}_{(G,S)}}$ induced by the Cayley graph $\mathcal{C}_{(G,S)}$ of a group G generated by a set S is connected and*

$$\begin{aligned} \dim_k \Lambda_{\mathcal{C}_{(G,S)}} &= |G||S|^2. \\ \dim_k Z(\Lambda_{\mathcal{C}_{(G,S)}}) &= 1 + \frac{|G||S|}{2}. \end{aligned} \quad (17)$$

Proof. $\Lambda_{\mathcal{C}_{(G,S)}}$ is connected as a consequence of Proposition 1, which states that the Cayley graph $\mathcal{C}_{(G,S)}$ is connected. On the other hand, we note that the Brauer configuration $\Gamma^{\mathcal{C}_{(G,S)}}$ induced by the Cayley graph $\mathcal{C}_{(G,S)}$ has non-truncated vertices, and the number of polygons $|\Gamma_1^{\mathcal{C}_{(G,S)}}|$ is $\frac{|G||S|}{2}$ provided that $\mathcal{C}_{(G,S)}$ is $|S|$ -regular.

Since the Brauer quiver $Q_{\mathcal{C}_{(G,S)}}$ has no loops, the Formula (17) holds as a consequence of Remark 2. We are finished. \square

As an example, we note that (see Figure 5)

$$\begin{aligned} \text{val}(x) &= 2 \text{ for all } x \in K, \quad |Q_1| = |\Gamma_0^{\mathcal{C}_{(K,\{a,b\})}}| = 4, \quad \#Loops(Q_{\mathcal{C}_{(K,\{a,b\})}}) = 0. \\ \dim_k \Lambda_{\mathcal{C}_{(K,\{a,b\})}} &= 2|Q_1| + 2(1)(4) = 16. \\ \dim_k Z(\Lambda_{\mathcal{C}_{(K,\{a,b\})}}) &= 1 + |Q_1| = 5. \end{aligned} \quad (18)$$

The following proposition gives the properties of the Brauer configuration algebra Λ_{B_n} induced by the butterfly graph B_n .

Proposition 2. *The Brauer configuration algebra Λ_{B_n} induced by an n -dimensional butterfly graph is connected and it holds that*

$$\begin{aligned} \dim_k \Lambda_{B_n} &= 2^n(16n - 10). \\ \dim_k Z(\Lambda_{B_n}) &= 1 + n2^{n+1}. \end{aligned} \quad (19)$$

Proof. Since B_n is connected, Λ_{B_n} is connected. Furthermore, Λ_{B_n} is reduced and the Brauer quiver induced by B_n has no loops. Formula (19) hold considering that if $(w, x) \in V_{B_n}$, then $\text{val}(w, x) = 2$ ($\text{val}(w, x) = 4$) if $x \in \{0, n\}$ ($1 \leq x \leq n - 1$) and $|E_{B_n}| = n2^{n+1}$. \square

Corollary 1 establishes relationships between the Brauer configuration algebras induced by pancake and star graphs.

Corollary 1. *For any $n > 2$, the Brauer configuration algebras Λ_{P_n} and Λ_{S_n} induced by the n th pancake graph and the n th star graph defined by the transposition graphs shown in Figure 3 are isomorphic.*

Proof. Since P_n and S_n are $(n - 1)$ -regular, connected graphs with $n!$ vertices, it holds that $\dim_K \Lambda_{P_n} = \dim_K \Lambda_{S_n}$ for any $n > 2$. \square

Figure 11 shows the butterfly graph B_2 and its induced Brauer quiver bounded by relations of the following types:

- $\alpha_i^a \alpha_j^a \alpha_i^a$, for all possible values of $i, j, a \in \{x_1, x_2, x_3, x_4, x'_1, x'_2, x'_3, x'_4\}$;
- $\alpha_{i_1}^b \alpha_{i_2}^b \alpha_{i_3}^b \alpha_{i_4}^b \alpha_{i_1}^b$, for all possible values of $i_1, i_2, i_3, i_4, b \in \{x'_1, x'_2, x'_3, x'_4\}$;
- $\alpha_i^x \alpha_j^y$, if $x \neq y$, for all possible values of i, j ;
- $C^a - C^b$, if a and b are endings of the same vertex $e \in E_{B_2}$ and C^x denotes a special cycle associated with the vertex $x \in V_{B_2}$.

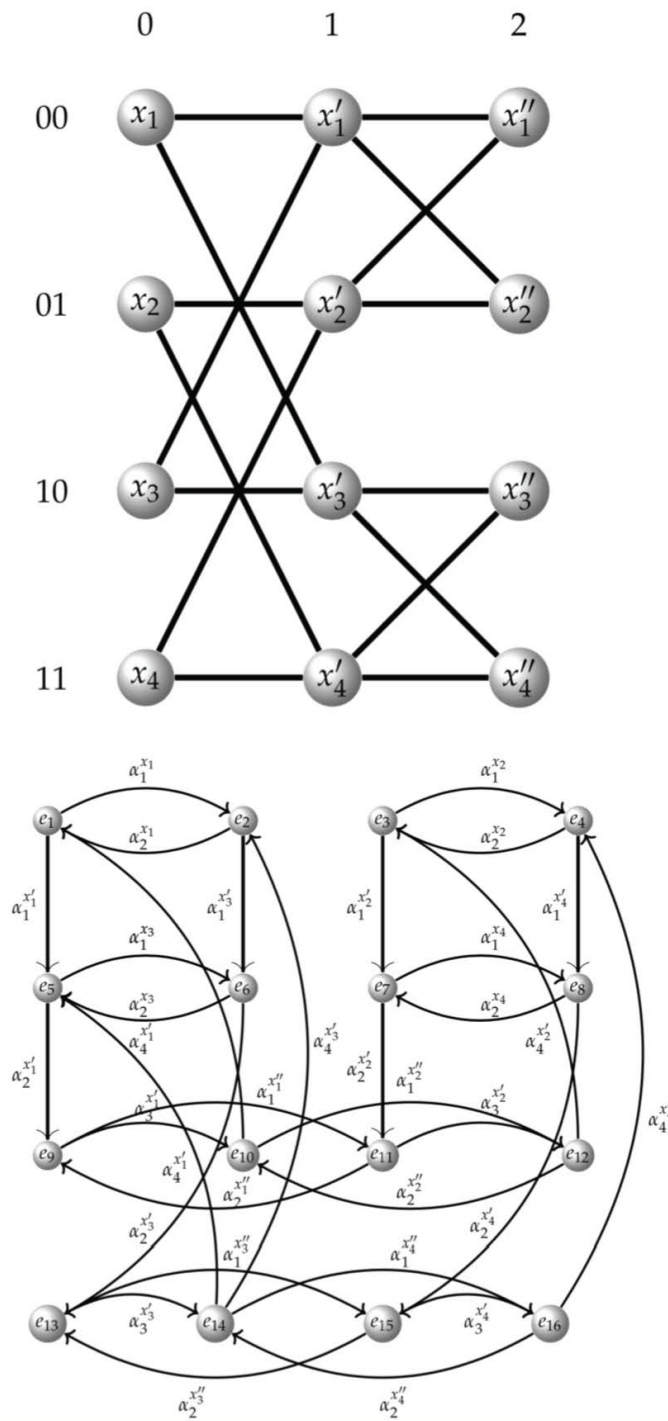


Figure 11. Butterfly graph B_2 and its induced Brauer quiver.

The successor sequences are given by the following identities:

$$\begin{aligned}
 S_{x_1} &= e_1 < e_2, & S_{x'_1} &= e_9 < e_{11}, \\
 S_{x_2} &= e_3 < e_4, & S_{x'_2} &= e_{10} < e_{12}, \\
 S_{x_3} &= e_5 < e_6, & S_{x'_3} &= e_{13} < e_{15}, \\
 S_{x_4} &= e_7 < e_8, & S_{x'_4} &= e_{14} < e_{16}, \\
 S_{x'_1} &= e_1 < e_5 < e_9 < e_{10}, \\
 S_{x'_2} &= e_3 < e_7 < e_{11} < e_{12}, \\
 S_{x'_3} &= e_2 < e_6 < e_{13} < e_{14}, \\
 S_{x'_4} &= e_4 < e_8 < e_{15} < e_{16}.
 \end{aligned}
 \tag{20}$$

Figure 12 shows the star graph ST_3 induced by the transposition graph shown in Figure 3 for $n = 3$.

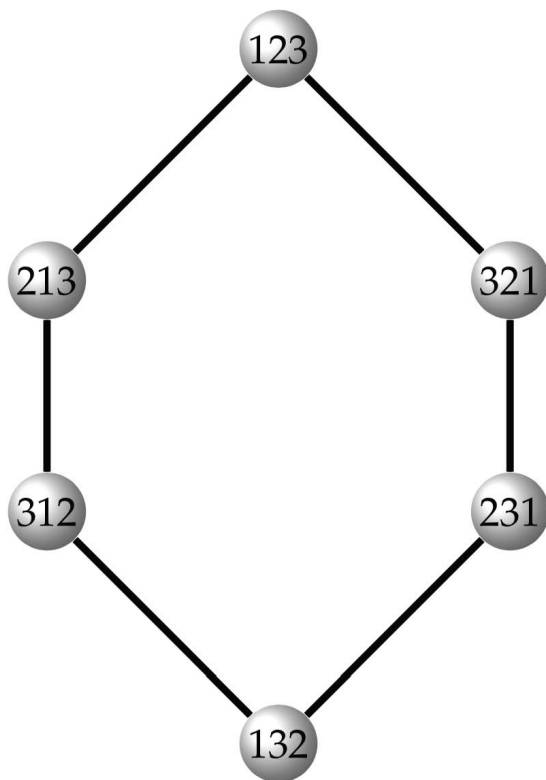


Figure 12. Star graph ST_3 defined by the transposition graph shown in Figure 3 for $n = 3$.

The following Theorem 2 defines Hamiltonian Brauer quivers.

Theorem 2. Let $\mathfrak{M} = (M, \mathfrak{M}_1, \mu, \mathcal{O})$ be a Brauer configuration for which

- \mathfrak{M}_1 is a collection of multisets $\{(M_1, f_1), (M_2, f_2), \dots, (M_n, f_n)\}$;
- $M = \bigcup_{i=1}^n (M_i, f_i)$;
- $\mu(x) = 1$ ($\mu(x) = 2$) if $val(x) > 1$ ($val(x) = 1$) for any $x \in M$;
- $(M_i, f_i) < (M_j, f_j)$ if $i < j$ in the successor sequences associated with the vertices;
- $N = \bigcap_{i=1}^n (M_i, f_i) \neq \emptyset$. For $1 \leq i \leq n$, $f_i(x) = 1$ if $x \in N$.

Then, the Brauer quiver $Q_{\mathfrak{M}}$ induced by the Brauer configuration \mathfrak{M} and bounded by relations of type (10) is Hamiltonian, and the number $h_{\mathfrak{M}}$ of Hamilton cycles is $h_{\mathfrak{M}} = n|N|$.

Proof. The successor sequence S_x of $x \in N$ has the form

$$S_x = M_1 < M_2 < \cdots < M_{n-1} < M_n \quad (21)$$

Then, S_x induces n non-disjunctive Hamiltonian paths in the Brauer quiver $Q_{\mathfrak{M}}$. On the other hand, since the product of the arrows in different successor sequences belongs to the ideal $I_{Q_{\mathfrak{M}}}$, it holds that $h_{\mathfrak{M}} = n|N|$. We are finished. \square

The following result proves that the transposition graph S_n gives rise to bounded Hamiltonian digraphs.

Corollary 2. Let Q_{S_n} be the Brauer quiver induced by the transposition graph of the star graph ST_n and bounded by relations of type (10) (see Figure 3 and Corollary 1); then, Q_{S_n} is Hamiltonian.

Proof. The successor sequence of the vertex $1 \in V_{S_n}$ has the form

$$S_1 = e_1 < e_2 \cdots < e_{n-2} < e_{n-1} \quad (22)$$

where $e_i = \{i, i+1\}$, $1 \leq i \leq n-1$. S_1 induces $n-1$ Hamiltonian paths in the Brauer quiver Q_{S_n} . \square

Corollary 3 gives closed formulas for the dimension of the Brauer configuration algebra induced by a transposition graph.

Corollary 3. Let Λ_{S_n} be the Brauer configuration algebra induced by the transposition graph of the star graph ST_n with $n > 2$; then,

$$\begin{aligned} \dim_k \Lambda_{S_n} &= n^2 - 1. \\ \dim_k Z(\Lambda_{S_n}) &= 2n - 1. \end{aligned} \quad (23)$$

Proof. Note that Q_{S_n} has $n-1$ vertices and $n-1$ loops, $val(1) = n-1$ and $val(j) = 1$, for any $j \neq 1$. Thus, $\dim_k \Lambda_{S_n} = 2(n-1) + (n-1)(n-2) + (n-1) = (n-1)(2+n-2+1) = (n-1)(n+1)$. Furthermore, $\dim_k Z(\Lambda_{S_n}) = 1 + 2(n-1) + 1 - n + n - 1 + n - 1 - n + 1 = 2n - 1$. We are finished. \square

3.2. Brauer Configuration Algebras Induced by Nilpotent Graphs

This section gives the properties of Brauer configuration algebras induced by nilpotent graphs defined by commutative rings of type \mathbb{Z}_n .

Theorem 3 and Corollary 4 give the properties of the Brauer configuration algebra $\Lambda_{\mathcal{N}(\mathbb{Z}_{2^n})}$ for $n > 1$.

Theorem 3. Let $\Lambda_{\mathcal{N}(\mathbb{Z}_{2^n})}$ be the Brauer configuration algebra induced by the nilpotent graph $\mathcal{N}(\mathbb{Z}_{2^n})$ over the commutative ring \mathbb{Z}_{2^n} , $n > 1$. Then, $\Lambda_{\mathcal{N}(\mathbb{Z}_{2^n})}$ satisfies the length grading property (see the fifth item of Remark 2) and

$$\begin{aligned} \dim_k \Lambda_{\mathcal{N}(\mathbb{Z}_{2^n})} &= 2t_{2^{n-1}-1} + 2^n t_{2^{n-1}-2}. \\ \dim_k Z(\Lambda_{\mathcal{N}(\mathbb{Z}_{2^n})}) &= 1 + t_{2^{n-1}-1}. \end{aligned} \quad (24)$$

Proof. Note that $\mathfrak{H}_{2^n} = \mathbb{Z}_{2^n} \setminus Nil(\mathbb{Z}_{2^n}) = \{2j-1 \mid 1 \leq j < 2^{n-1}\}$; then, if $i, j \in \mathfrak{H}_{2^n}$ and $i \neq j$; then, $i = 2k_i - 1$ and $j = 2k_j - 1$ and $i+j \in Nil(\mathbb{Z}_{2^n})$. Therefore, they can be connected by an edge $e \in E_{\mathcal{N}(\mathbb{Z}_{2^n})}$. Thus, $\mathcal{N}(\mathbb{Z}_{2^n})$ is complete, its induced Brauer quiver is connected and the corresponding Brauer configuration is reduced. Since $val(j) = 2^{n-1} - 1$, for any $j \in V_{\mathcal{N}(\mathbb{Z}_{2^n})}$, then $\Lambda_{\mathcal{N}(\mathbb{Z}_{2^n})}$ has the length grading property.

We also note that a typical successor sequence S_{2j-1} induced by the Brauer configuration $\Gamma^{\mathcal{N}(\mathbb{Z}_{2^n})}$ has the form

$$S_{2j-1} = (2j - 1, 1) < \dots < (2j - 1, 2j - 3) < (2j - 1, 2j + 1) < \dots < (2j - 1, 2^n - 1). \tag{25}$$

where $(2j - 1, h) \in E_{\mathcal{N}(\mathbb{Z}_{2^n})}$, $(2j - 1, h) \in S_h$, if $h < 2j - 1$. Then, $\mathcal{N}(\mathbb{Z}_{2^n})$ has $t_{2^{n-1}-1}$ edges and 2^{n-1} vertices. Therefore, $\dim_k \Lambda_{\mathcal{N}(\mathbb{Z}_{2^n})} = 2t_{2^{n-1}-1} + 2^{n-1}(2^{n-1} - 1)(2^{n-1} - 2) = 2t_{2^{n-1}-1} + 2^n t_{2^{n-1}-2}$. Furthermore, $\dim_k Z(\Lambda_{\mathcal{N}(\mathbb{Z}_{2^n})}) = 1 + t_{2^{n-1}-1}$ provided that $\mathcal{N}(\mathbb{Z}_{2^n})$ has no loops. \square

The following Corollary proves that Brauer quivers of type $Q_{\mathcal{N}(\mathbb{Z}_{2^n})}$ are not Hamiltonian.

Corollary 4. *Let $Q_{\mathcal{N}(\mathbb{Z}_{2^n})}$ be the Brauer quiver induced by the nilpotent graph $\mathcal{N}(\mathbb{Z}_{2^n})$; then, $Q_{\mathcal{N}(\mathbb{Z}_{2^n})}$ is not Hamiltonian for all positive integers n .*

Proof. The longest cycle in $Q_{\mathcal{N}(\mathbb{Z}_{2^n})}$ has $2^{n-1} - 1$ arrows and $|V_{Q_{\mathcal{N}(\mathbb{Z}_{2^n})}}| = t_{2^{n-1}-1} = \frac{2^{n-1}(2^{n-1}-1)}{2}$. We are finished. \square

As an example, the following are the successor sequences induced by the nilpotent graph $\mathcal{N}(\mathbb{Z}_8)$ shown in Figure 13. Brauer quivers $Q_{\mathcal{N}_{\mathbb{Z}_8}}$ and $Q_{\mathcal{N}_{\mathbb{Z}_{16}}}$ induced by $\mathcal{N}(\mathbb{Z}_8)$ and $\mathcal{N}(\mathbb{Z}_{16})$ are shown in Figures 13 and 14, respectively.

$$\begin{aligned} S_1 &= (1, 3) < (1, 5) < (1, 7). \\ S_3 &= (3, 1) < (3, 5) < (3, 7). \\ S_5 &= (5, 1) < (5, 3) < (5, 7). \\ S_7 &= (7, 1) < (7, 3) < (7, 5). \end{aligned} \tag{26}$$

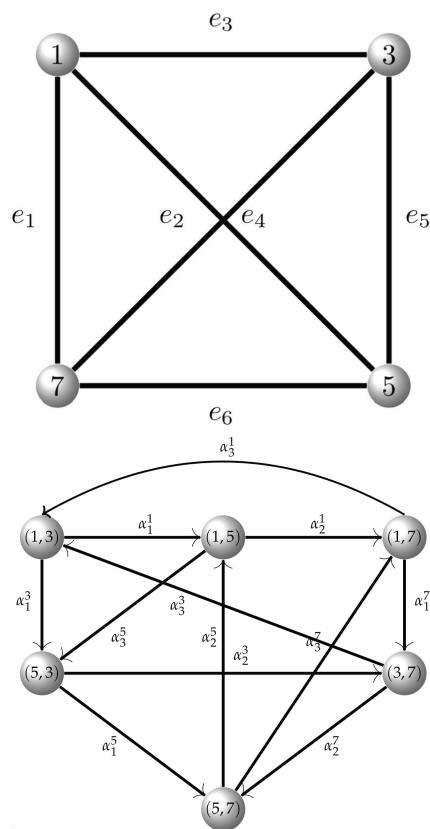


Figure 13. Nilpotent graph $\mathcal{N}(\mathbb{Z}_8)$ and its induced Brauer quiver $Q_{\mathcal{N}(\mathbb{Z}_8)}$.

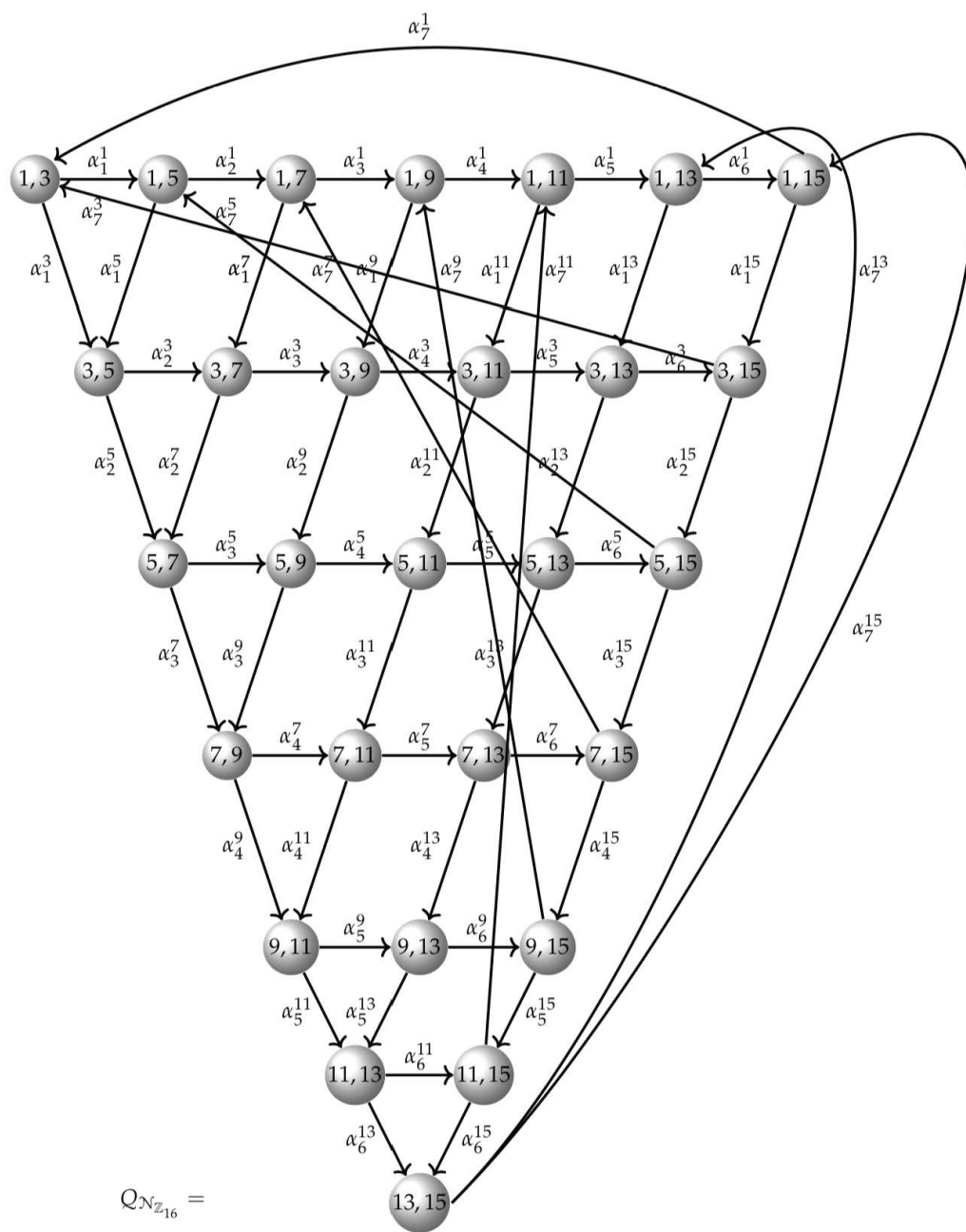


Figure 14. Brauer quiver $Q_{N(\mathbb{Z}_{16})}$ induced by the nilpotent graph $N(\mathbb{Z}_{16})$.

The Brauer quiver $Q_{N(\mathbb{Z}_{2^n})}$, $n > 1$, is bounded by relations of the following form.

- $\alpha_{i_1}^a \alpha_{i_2}^a \dots \alpha_{i_{2^n-1-1}}^a - \alpha_{j_1}^b \alpha_{j_2}^b \dots \alpha_{j_{2^n-1-1}}^b$, for all possible values of i_k, j_k , $k \in \{1, 2, \dots, 2^n - 1\}$, $\{a, b\} \in E_{N(\mathbb{Z}_{2^n})}$.
- $\alpha_{i_1}^a \alpha_{i_2}^a \dots \alpha_{i_{2^n-1-1}}^a \alpha_{i_1}^a$, for all possible values of i_k , $a \in \{1, 3, 5, \dots, 2^n - 1\}$.
- $\alpha_i^a \alpha_j^b$, if $a \neq b$, $a, b \in \{1, 3, 5, \dots, 2^n - 1\}$.

Theorem 4 gives a closed formula for the dimension of a Brauer configuration algebra induced by the commutative ring $\mathbb{Z}_{2^n p_1 p_2 \dots p_s}$, where p_j is an odd prime number.

Theorem 4. Let $\Lambda_{\mathcal{N}(\mathbb{Z}_t)}$ be the Brauer configuration algebra induced by the nilpotent graph $\mathcal{N}(\mathbb{Z}_t)$ with $t = 2^n p_1 p_2 \dots p_s$, $n > 1$, p_j an odd prime number for each $1 \leq j \leq s$, $p_i \neq p_j$ if $i \neq j$. Then,

$$\dim_k \Lambda_{\mathcal{N}(\mathbb{Z}_t)} = 2|Q_1| + 2^{n+1}(p_1 p_2 \dots p_k - 1)t_{2^{n-1}-1} + 2^n t_{2^{n-1}-2}. \quad (27)$$

where $|Q_1| = (p_1 p_2 \dots p_s - 1)2^{n-1} + (2p_1 p_2 \dots p_s - 1)t_{2^{n-1}-1}$.

Proof. Firstly, we note that $|\text{Nil}(\mathbb{Z}_t)| = 2^{n-1}$. In fact, if $h = 2p_1 p_2 \dots p_s$, then $\text{Nil}(\mathbb{Z}_t) = \{jh \mid 1 \leq j \leq 2^{n-1}\}$.

Let $\Gamma^{\mathcal{N}(\mathbb{Z}_t)}$ be the Brauer configuration defined by the nilpotent graph $\mathcal{N}(\mathbb{Z}_t)$; then, according to Remark 3, it holds that

$$\begin{aligned} |\{\alpha \in \Gamma_0^{\mathcal{N}(\mathbb{Z}_t)} \mid \text{val}(\alpha) = 2^{n-1}\}| &= 2^n(h/2 - 1). \\ |\{\alpha \in \Gamma_0^{\mathcal{N}(\mathbb{Z}_t)} \mid \text{val}(\alpha) = 2^{n-1} - 1\}| &= 2^{n-1}. \\ |E_{\mathcal{N}(\mathbb{Z}_t)}| &= |Q_1|. \end{aligned} \quad (28)$$

$|Q_1|$ can be found by building successor sequences as in the proof of Theorem 3 and enumerating their edges without taking into account repetitions. In such a case, we note that there are $h/2 - 1$ successor sequences with 2^{n-1} edges, and $h - 1$ sequences with $2^{n-1} - j$ edges, $1 \leq j \leq 2^{n-1} - 1$. Then,

$$|Q_1| = (h/2 - 1)2^{n-1} + (h - 1)t_{2^{n-1}-1}. \quad (29)$$

Thus,

$$\dim_k \Lambda_{\mathcal{N}(\mathbb{Z}_t)} = 2|Q_1| + 2^n(h/2 - 1)(2^{n-1})(2^{n-1} - 1) + 2^{n-1}(2^{n-1} - 1)(2^{n-1} - 2) = 2|Q_1| + 2^{n+1}(h/2 - 1)t_{2^{n-1}-1} + 2^n t_{2^{n-1}-2}. \quad \square$$

The following result gives a closed formula for the dimension of a Brauer configuration algebra induced by a graph $\mathcal{N}(\mathbb{Z}_{p_1^{a_1} p_2^{a_2} \dots p_t^{a_t}})$, where p_j , $1 \leq j \leq t$ is an odd prime number and a_i is a positive integer $1 \leq i \leq t$.

Theorem 5. Let $\Lambda_{\mathcal{N}(\mathbb{Z}_n)}$ be a Brauer configuration algebra induced by the nilpotent graph $\mathcal{N}(\mathbb{Z}_n)$, where \mathfrak{p} is a product of the form $n = p_1^{a_1} p_2^{a_2} \dots p_t^{a_t}$, where, for each $1 \leq j \leq t$, a_j is a positive integer and p_j is an odd prime number, $p_i \neq p_j$ if $i \neq j$. Then,

$$\dim_k \Lambda_{\mathcal{N}(\mathbb{Z}_n)} = 2 \lfloor \frac{\mathfrak{p}}{2} \rfloor |\text{Nil}(\mathbb{Z}_n)| (|\text{Nil}(\mathbb{Z}_n)| + 2t_{|\text{Nil}(\mathbb{Z}_n)|-1}). \quad (30)$$

where $\mathfrak{p} = p_1 p_2 \dots p_t$.

Proof. It is a consequence of the results mentioned in Remark 3. Firstly, we note that $|V_{\mathcal{N}(\mathbb{Z}_n)}| = 2|\text{Nil}(\mathbb{Z}_n)| \lfloor \frac{\mathfrak{p}}{2} \rfloor$ and $|E_{\mathcal{N}(\mathbb{Z}_n)}| = |\text{Nil}(\mathbb{Z}_n)|^2 \lfloor \frac{\mathfrak{p}}{2} \rfloor$. Since $\text{val}(x) = |\text{Nil}(\mathbb{Z}_n)|$ for any $x \in V_{\mathcal{N}(\mathbb{Z}_n)}$, it holds that

$$\dim_k \Lambda_{\mathcal{N}(\mathbb{Z}_n)} = 2|\text{Nil}(\mathbb{Z}_n)|^2 \lfloor \frac{\mathfrak{p}}{2} \rfloor + 4|\text{Nil}(\mathbb{Z}_n)| \lfloor \frac{\mathfrak{p}}{2} \rfloor t_{|\text{Nil}(\mathbb{Z}_n)|-1}. \quad (31)$$

We are finished. \square

The following Corollary gives a closed formula for the dimension of a Brauer configuration algebra induced by components of some disconnected nilpotent graphs.

Corollary 5. Let $\Lambda_{\kappa(\mathcal{N}(\mathbb{Z}_n))}$ be a Brauer configuration algebra induced by a component of the nilpotent graph $\mathcal{N}(\mathbb{Z}_n)$ mentioned in Theorem 5. Then,

$$\dim_k Z(\Lambda_{\kappa(\mathcal{N}(\mathbb{Z}_n))}) = 1 + |\text{Nil}(\mathbb{Z}_n)|^2. \quad (32)$$

Proof. The Brauer configuration $\Gamma^{\mathcal{N}(\mathbb{Z}_n)}$ induced by the nilpotent graph $\mathcal{N}(\mathbb{Z}_n)$ is reduced and the corresponding Brauer quiver has no loops. The result follows taking into account that $|E(\kappa(\mathcal{N}(\mathbb{Z}_n)))| = |\text{Nil}(\mathbb{Z}_n)|^2$. We are finished. \square

3.3. Brauer Configuration Algebras Induced by Quantum Entanglements

This section describes the properties of the Brauer configuration algebras induced by the experimental setups developed by Zeilinger et al. [28–30] to derive quantum entanglement states of type GHZ , W_n and D_n^m .

The following theorem gives the property of the Brauer configuration algebras induced by setups of type GHZ_n^2 given by Zeilinger et al. We let $\mathcal{M}^{GHZ_n^2}$ denote the Brauer configuration induced by a setup of type GHZ_n^d and $\#Crystals$ the number of crystals in the GHZ_n^2 setup.

Theorem 6. *Setups of type GHZ_n^2 ($n \geq 4$) induce Brauer configuration algebras $\Lambda_{GHZ_n^2}$ with the following properties.*

1. $\Lambda_{GHZ_n^2}$ is connected.
2. $\Lambda_{GHZ_n^2}$ has the length grading property.
3. $\dim_k \Lambda_{GHZ_n^2} = 4\#Crystals$, where k is an algebraically closed field.
4. $\dim_k Z(\Lambda_{GHZ_n^2}) = 1 + \#Crystals$.
5. The Brauer message of a labeled Brauer configuration $M(\mathcal{M}^{GHZ_n^2})$ is the undirected graph C_n ($n \geq 4$ is an even integer), whose edges are labeled by the states $|00\rangle$ and $|11\rangle$.
6. If, in Remark 1 and Formulas (5) and (6), it holds that each term F_j corresponds to a unique labeled perfect matching of C_n obtained by applying a tensor product to its labels (i.e., $O_{h_j} = \otimes$ for all F_j) and O_s is the usual sum in (6), then $M^e(\mathcal{M}^{GHZ_n^2})/\sqrt{2} = |GHZ_n^2\rangle$.

Proof.

1. Firstly, we note that the Brauer configuration $\mathcal{M}^{GHZ_n^2} = (M_0^{GHZ_n^2}, M_1^{GHZ_n^2}, \mu, \mathcal{O})$ has particles as a set of vertices $M_0^{GHZ_n^2} = \{a_1, a_2, \dots, a_n\}$. The word-polygons in $M_1^{GHZ_n^2}$ are given by path particle coincidences. Therefore, if $M_j \in M_1^{GHZ_n^2}$, then $w(M_j) = a_{j_1}a_{j_2}$, which means that there are two paths containing particles $a_{j_1}, a_{j_2} \in M_0^{GHZ_n^2}$. $\mu(a_j) = 1$ for any $a_j \in M_0^{GHZ_n^2}$. Furthermore, if $M_r = \{a_{r_1}, a_{r_2}\} \in M_1^{GHZ_n^2}$, $M_s = \{a_{s_1}, a_{s_2}\} \in M_1^{GHZ_n^2}$, then $M_r < M_s$ in the successor sequences if $a_{r_1} = a_{s_1}$ and $r_2 < s_2$ (the set of indices is endowed with the usual order of natural numbers) or $a_{r_1} = a_{s_2}$ and $r_2 < s_1$. Using the same arguments, we adopt ordering $\{M_r, M_s\}$ via $a_{r_2} \in M_r$. Since the undirected graph associated with the state $|GHZ_n^2\rangle$ is connected and its edges are in correspondence with the polygons in $M_1^{GHZ_n^2}$, we conclude that $\mathcal{M}^{GHZ_n^2}$ is connected.
2. $val(a_j)\mu(a_j) = 2$ for any particle $a_j \in M_0^{GHZ_n^2}$.
3. Since the number of crystals $\#Crystals$ used by Zeilinger et al. in their GHZ_n^2 setup equals $|M_1^{GHZ_n^2}|$ and $val(a_j) = 2$, for any $a_j \in M_0^{GHZ_n^2}$, it holds that $\dim_k \Lambda_{\mathcal{M}^{GHZ_n^2}} = 2|M_1^{GHZ_n^2}| + 2(1)|M_1^{GHZ_n^2}| = 4\#Crystals$.
4. The connected Brauer quiver $\mathcal{Q}_{\mathcal{M}^{GHZ_n^2}}$ induced by the Brauer configuration $\mathcal{M}^{GHZ_n^2}$ has no loops and $val(a_j) = 2$ for any $a_j \in M_0^{GHZ_n^2}$. Therefore, $\dim_k Z(\Lambda_{GHZ_n^2}) = 1 + |M_1^{GHZ_n^2}| = 1 + \#Crystals$.
5. Words defined by polygons in $M_1^{GHZ_n^2}$ are given by path particle coincidences. Then, we define an unoriented graph $\mathcal{G}_{GHZ_n^2} = (\mathcal{V}_{GHZ_n^2}, \mathcal{E}_{GHZ_n^2})$ with $\mathcal{V}_{GHZ_n^2} = M_0^{GHZ_n^2}$ and $\mathcal{E}_{GHZ_n^2} = M_1^{GHZ_n^2}$. In this case, two of these words $w(M_i) = a_{i_1}a_{i_2}$ and $w(M_j) =$

$a_{j_1} a_{j_2}$ are concatenated if $M_i \cap M_j \neq \emptyset$. In such a case, a two-word concatenation $w(M_i)w(M_j)$ defines a path in $\mathcal{G}_{GHZ_n^d}$ and the message $M(\mathcal{M}^{GHZ_n^2})$ obtained via such concatenation gives $\mathcal{G}_{GHZ_n^2}$. Since each coincidence corresponds to the mode number of a photon state, it labels the corresponding polygon (edge in $\mathcal{E}_{GHZ_n^2}$).

- Perfect matching $PM(\mathcal{G}_{GHZ_n^2})$ gives a partition $\mathcal{F} = \{F_1, F_2, \dots, F_p\}$ of $M_1^{GHZ_n^2}$. Each specialized word $w^{\epsilon(F_j)}$ is the tensor product of its edge labels. Then,

$$M^\epsilon(\mathcal{M}^{GHZ_n^2}) = F_1 + F_2 + \dots + F_p = \sqrt{2}|GHZ_n^2\rangle. \tag{33}$$

□

As an example, note that the Brauer quiver $Q_{C(K,S)}$ shown in Figure 5 and induced by the four Klein group is isomorphic to the Brauer $Q_{\mathcal{M}^{GHZ_4^2}}$ induced by the quantum entanglement setup GHZ_4^2 .

The following result is a version of Theorem 6 for generalized GHZ_n^3 setups. We recall that the case GHZ_4^3 is the only one that has been experimentally developed.

Theorem 7. *Setups of type GHZ_n^3 ($n \geq 4$) induce Brauer configuration algebras $\Lambda_{GHZ_n^3}$ with the following properties.*

- $\Lambda_{GHZ_n^3}$ is connected.
- $\Lambda_{GHZ_n^3}$ has the length grading property.
- $\dim_k \Lambda_{GHZ_n^3} = \#Crystals + 6\#particles$, where k is an algebraically closed field.
- $\dim_k Z(\Lambda_{GHZ_n^3}) = 1 + \#Crystals$.
- The Brauer message of a labeled Brauer configuration $M(\mathcal{M}^{GHZ_n^3})$ is the undirected graph $\mathcal{G}_{GHZ_n^3}$ obtained via the concatenation of consecutive complete graphs K_4 (see Figures 15 and 16) whose edges are labeled by the states $|00\rangle, |11\rangle$ and $|22\rangle$.
- If the hypothesis in the sixth item of Theorem 6 holds for the graph $\mathcal{G}_{GHZ_n^3}$, then $M^\epsilon / \sqrt{3} = |GHZ_n^3\rangle$.

Proof. Similar constructions as those used in the proof of items (1), (2), (4), (5) and (6) prove that the Brauer configuration $\mathcal{M}^{GHZ_n^3} = (M_0^{GHZ_n^3}, M_1^{GHZ_n^3}, \mu, \mathcal{O})$ is connected, the corresponding algebra $\Lambda_{GHZ_n^3}$ has the length grading property and $M^\epsilon(\mathcal{M}^{GHZ_n^3}) / \sqrt{3} = |GHZ_n^3\rangle$. Moreover, $\mathcal{M}_0^{GHZ_n^3}$ has non-truncated vertices and the Brauer quiver $Q_{\mathcal{M}^{GHZ_n^3}}$ has no loops.

We also note that $|M_1^{GHZ_n^3}| = \#Crystals = 6 + 5(j - 2)$, if $n = 2j$. Furthermore, $\mu(a_j) = 1$ and $val(a_j) = 3$, for any $a_j \in M_0^{GHZ_n^3}$. □

Figures 15 and 16 show a generalized setup of type GHZ_n^3 and its induced graph $\mathcal{G}_{GHZ_n^3}$. The number of perfect matchings $\#PM(\mathcal{G}_{GHZ_n^3})$ of the graph $\mathcal{G}_{GHZ_n^3}$ is given by the so-called Jacobsthal sequence $J_n = \frac{2^n - (-1)^n}{3} = \{0, 1, 1, 3, 5, 11, \dots\}$, $n \geq 0$ (A001045 in the Online Encyclopedia of Integer Sequences (OEIS) [46]).

Theorem 8 concerns Brauer configuration algebras induced by setups of type $D_n^1 = W_n$. We assume the notation a_1, a_2, \dots, a_n for particles and that one crystal produces two-photon pairs in states $|01\rangle$ and $|10\rangle$.

Paths associated with particles a_1 and a_2 are the only containing such a crystal. Defining, in this way, two identical word-polygons with different labels $M_1 = (a_1 a_2; |10\rangle)$ and $M_2 = (a_1 a_2; |01\rangle)$, we let L_x denote the path length associated with a particle x in a setup of type W_n .

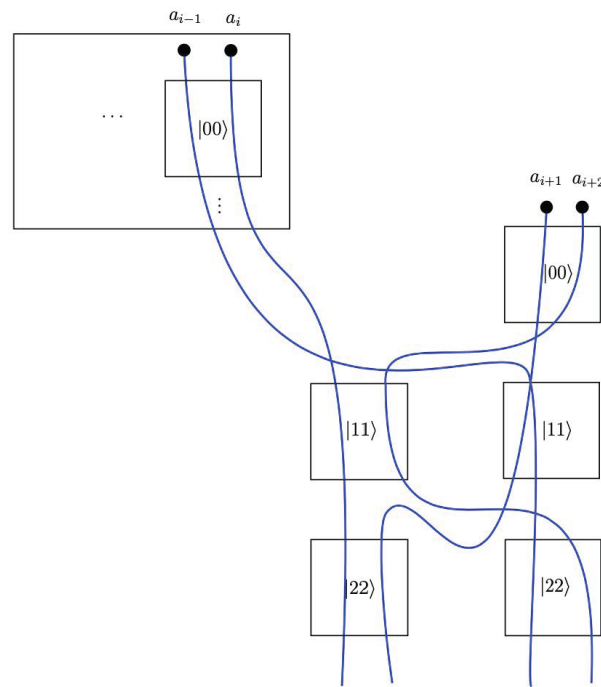


Figure 15. Generalized setup of type GHZ_n^3 .

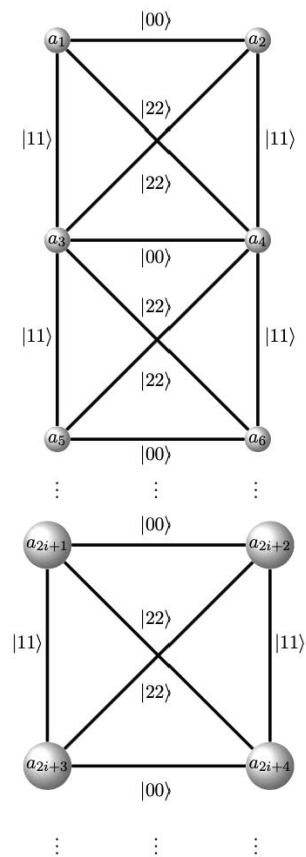


Figure 16. The graph $\mathcal{G}_{GHZ_n^3}$ induced by a generalized setup of type GHZ_n^3 .

Theorem 8. *Setups of type W_n ($n \geq 4$) induce Brauer configuration algebras Λ_{W_n} with the following properties.*

1. Λ_{W_n} is connected.

2. $\dim_k \Lambda_{W_n} = 2(\#Crystals + 1) + 4t_{\#particles-1} + 6(\#particles - 2)$.
3. $\dim_k Z(\Lambda_{W_n}) = \#Crystals + 2$.
4. The Brauer message of a labeled Brauer configuration $M(\mathcal{M}^{W_n})$ is the undirected graph $P_2 \times S_n$ whose edges are labeled by the states $|10\rangle$ and $|01\rangle$, where P_2 is the two-vertex path graph and S_n is an n -vertex transposition graph (see Figure 3).
5. If the hypothesis in the sixth item of Theorem 6 holds for $P_2 \times S_n$, then $M^\varepsilon(\mathcal{M}^{W_n})/\sqrt{n} = |W_n\rangle$.

where $t_j = \frac{j(j-1)}{2}$ denotes the j th triangular number.

Proof.

1. The Brauer configuration $\mathcal{M}^{W_n} = (\mathcal{M}_0^{W_n}, \mathcal{M}_1^{W_n}, \mu, \mathcal{O})$ induced by a setup W_n ($n \geq 4$ is a fixed even integer) has the particles as a set of vertices $\mathcal{M}_0^{W_n} = \{a_1, a_2, \dots, a_n\}$, and word-polygons are defined by path coincidences. There are two polygons $M_1 = (a_1 a_2; |10\rangle)$ and $M_2 = (a_1 a_2; |01\rangle)$ defined by the same words with different labels. Since $(a_1 a_i; |x_{1,1} x_{1,2}\rangle), (a_1 a_j; |x_{2,1} x_{2,2}\rangle) \in \mathcal{M}_1^{W_n}$, with $1 \leq i, j \leq n$, $|x_{1,1} x_{1,2}\rangle = |x_{2,1} x_{2,2}\rangle = |10\rangle$ if $i = 2$ and $j = 1$, $|x_{1,1} x_{1,2}\rangle = |x_{2,1} x_{2,2}\rangle = |01\rangle$, otherwise. The remaining word-polygons have the form $(a_r a_s; |01\rangle)$, $r, s \notin \{1, 2\}$, where $a_r a_s$ is an edge of the undirected graph induced by the setup. Furthermore, $\mu(a_j) = 1$ for any $a_j \in \mathcal{M}_0^{W_n}$. The order in the successor sequences is given as in the proof of Theorem 6. These constructions allow us to conclude that the Brauer configuration \mathcal{M}^{W_n} is connected.
2. We note that $\mathcal{M}_1^{W_n}$ contains polygon-words of the form $(a_1 a_i; |x_{1,1} x_{1,2}\rangle), (a_2 a_j; |x_{2,1} x_{2,2}\rangle)$, $1 \leq i, j \leq n$. Thus, $|\mathcal{M}_1^{W_n}| = \#Crystals + 1$, $val(a_1) = val(a_2) = n = \#particles$. The remaining $(\#particles - 2)$ -vertices have valency 3 (note that the undirected graph induced by the setup is given by a graph product of the form $P_2 \times S_{n/2}$, where $S_{n/2}$ is a transposition graph (see Figure 3)). The formula holds provided that $\mu(a_j) = 1$ for any particle $a_j \in \mathcal{M}_0^{W_n}$.
3. The Brauer configuration \mathcal{M}^{W_n} is connected, $\mathcal{M}_0^{W_n}$ consists of non-truncated vertices, and the induced Brauer quiver $Q_{\mathcal{M}^{W_n}}$ has no loops. The formula follows as a consequence of the seventh item of Remark 2.
4. Words $a_i a_j$ associated with polygons of the form $(a_i a_j; |x_{1,1} x_{1,2}\rangle) \in \mathcal{M}_1^{W_n}$ are given by path-particle coincidences. Therefore, their concatenation defines an unoriented graph $\mathcal{G}_{W_n} = (\mathcal{V}_{W_n}, \mathcal{E}_{W_n})$ with $\mathcal{V}_{W_n} = \mathcal{M}_0^{W_n}$ and $\mathcal{E}_{W_n} = \mathcal{M}_1^{W_n}$. Since the concatenation is defined as in Theorem 6, it defines the undirected graph of the form $P_2 \times S_n$ whose edges are labeled by photon states $|10\rangle$ and $|01\rangle$.
5. This result holds by applying to the graph \mathcal{G}_{W_n} similar arguments as in the proof of Theorem 6.

□

The following result concerns the $D_n^{n/2}$ setups introduced by Zeilinger et al. [28–30] to derived Dicke states of type $|D_n^{n/2}\rangle$ via the perfect matchings of its associated graph.

Corollary 6. Let $\Lambda_{D_n^{n/2}}$ be the Brauer configuration algebra induced by a setup of type $D_n^{n/2}$ and a Brauer configuration $\mathcal{M}^{D_n^{n/2}} = (\mathcal{M}_0^{D_n^{n/2}}, \mathcal{M}_1^{D_n^{n/2}}, \mu, \mathcal{O})$, whose set of vertices $\mathcal{M}_0^{D_n^{n/2}}$, labeled word-polygons $\mathcal{M}_1^{D_n^{n/2}}$, vertex-multiplicity μ and orientation \mathcal{O} are defined as in Theorems 6–8, where labeled words have the forms $(a_i a_j; |10\rangle)$ and $(a_i a_j; |01\rangle)$, $1 \leq i, j \leq n$. Then, for $n \geq 4$ fixed, the Brauer configuration algebra $\Lambda_{D_n^{n/2}}$ satisfies the following properties.

1. $\Lambda_{D_n^{n/2}}$ is connected.
2. $\Lambda_{D_n^{n/2}}$ has the length grading property.
3. $\dim_k \Lambda_{D_n^{n/2}} = 4(\#Crystals) + (\#particles)t_{2\#particles-3}$.

4. $\dim_k Z(\Lambda_{D_n^{n/2}}) = 2\#\text{Crystals} + 1$.
5. The Brauer message of a labeled Brauer configuration $M(\mathcal{M}^{D_n^{n/2}})$ is the undirected complete graph \underline{K}_n whose vertices (particles) are connected by doubled edges (of the complete graph K_n) labeled by the states $|10\rangle$ and $|01\rangle$.
6. If the hypothesis in the sixth item of Theorem 6 holds for \underline{K}_n , then $M^\epsilon(\mathcal{M}^{D_n^{n/2}})/\sqrt{n} = |D_n^{n/2}\rangle$.

Proof.

1. We note that, by definition, if $a_i, a_j \in \mathcal{M}_0^{D_n^{n/2}}$, then there is a crystal $e_{i,j}$ where their corresponding paths L_{a_i} and L_{a_j} coincide.
2. $val(a_i)\mu(a_i) = 2(\#\text{particles} - 1)$, for any particle $a_i \in \mathcal{M}_0^{D_n^{n/2}}$.
3. It suffices to note that $|\mathcal{M}_1^{D_n^{n/2}}| = 2\#\text{Crystals}$.
4. The result holds provided that the Brauer quiver $Q_{\mathcal{M}^{D_n^{n/2}}}$ has no loops and $val(a_j) > 1$ for any $a_j \in \mathcal{M}_0^{D_n^{n/2}}$.
5. Polygon-words and their concatenation (where two words (edges) are connected provided that they have a common vertex) give an unoriented graph $M(\mathcal{M}^{D_n^{n/2}}) = (V_{D_n^{n/2}}, E_{D_n^{n/2}})$, $V_{D_n^{n/2}} = \mathcal{M}_0^{D_n^{n/2}}$ and $E_{D_n^{n/2}} = \mathcal{M}_1^{D_n^{n/2}}$. Thus, $M(\mathcal{M}^{D_n^{n/2}})$ is nothing but the graph induced by the setup $D_n^{n/2}$.
6. As in Theorem 6, the labels associated with the perfect matchings of $M(\mathcal{M}^{D_n^{n/2}})$ give $|D_n^{n/2}\rangle$.

□

4. Conclusions

Cayley and nilpotent graphs induce Brauer configuration algebras. If a subset S generates a group G , the induced Brauer configuration algebra satisfies the length grading property, and closed formulas for their dimensions and center can be obtained. The same can be proven for Brauer configuration algebras induced by commutative rings of the form \mathbb{Z}_{2^n} . In particular, it is possible to prove that some Cayley graphs give rise to Hamiltonian Brauer quivers.

Although Brauer configuration algebras induced by butterfly graphs do not satisfy the length grading property, such algebras are connected and reduced, and it is possible to obtain closed formulas for their dimensions. These results prove that some Brauer configuration algebras induced by pancake and star graphs are isomorphic.

Since quantum entangled states GHZ_n^2 , GHZ_n^3 and W_n give rise to undirected graphs, we conclude that such quantum states induce Brauer configuration algebras whose dimensions depend on the number of crystals used in the corresponding setups.

Future Work

1. This paper gives closed formulas for Brauer configuration algebras induced by some nilpotent graphs. It would be an interesting task for the future to give closed formulas (or to perform a Brauer analysis) for the dimensions of all Brauer configuration algebras induced by commutative rings of type \mathbb{Z}_n .
2. Another task for the future is to determine which Cayley graphs induce Hamiltonian Brauer quivers.
3. In the future, the experimental construction of generalized quantum entangled states will allow the existence of suitable Brauer configuration algebras.

Author Contributions: Investigation, writing, review and editing, A.M.C., I.G. and O.M.M. All authors have read and agreed to the published version of the manuscript.

Funding: Convocatoria Nacional para el Establecimiento de Redes de Cooperación bajo el Marco del Modelo Intersedes 2022–2024, Universidad Nacional de Colombia. Proyecto: Interacciones entre

el álgebra, la combinatoria y la computación cuántica con aplicaciones en ciberseguridad y análisis topológico de datos. Cod Hermes 59773.

Data Availability Statement: Data are contained within the article.

Conflicts of Interest: The authors declare no conflicts of interest.

Abbreviations

The following abbreviations are used in this manuscript:

$\#Crystals$	Number of crystals in a quantum entanglement setup
$\dim_k \Lambda_{\mathcal{G}}$	Dimension of a Brauer configuration algebra
$ D_n^m\rangle$	Dicke entanglement state
$\lfloor x \rfloor$	Greatest integer less than an inter number x
$ GHZ_n^d\rangle$	Greenberger–Horne–Zeilinger entanglement state
$\Lambda_{\mathcal{G}}$	Brauer configuration algebra induced by the graph \mathcal{G}
$Nil(\mathbb{Z}_n)$	Set of nilpotent elements of the ring \mathbb{Z}_n
$\#particles$	Number of particles in a quantum entanglement setup
P_n	Pancake graph
ST_n	Star graph
$ X $	Size of a set X
t_i	i th triangular number
$val(x)$	Valency of a vertex x
$ W_n\rangle$	Dicke entanglement state $ D_n^1\rangle$
$\lfloor x \rfloor$	Greatest integer less than an inter number x
$Z(\Lambda_{\mathcal{G}})$	Center of a Brauer configuration algebra

References

- Cayley, A. Desiderata and suggestions No. 2. The theory of groups: Graphical representation. *Am. J. Math.* **1878**, *1*, 174–176. [\[CrossRef\]](#)
- Beck, I. Coloring of commutative rings. *J. Algebra* **1988**, *116*, 208–226. [\[CrossRef\]](#)
- Anderson, D.F.; Livingston, P.S. The zero-divisor graph of a commutative ring. *J. Algebra* **1999**, *217*, 434–477. [\[CrossRef\]](#)
- Kala, R.; Kavhita, S. A typical graph structure of a ring. *Trans. Comb* **2015**, *116*, 37–44.
- Khojasteh, S.; Nikmehr, M.J. The weakly nilpotent graph of a commutative ring. *Canad. Math. Bull.* **2017**, *60*, 319–328. [\[CrossRef\]](#)
- Basnet, D.K.; Sharma, A.; Dutta, R. Nilpotent graph. *Theory Appl. Graphs* **2021**, *8*, 1–9. [\[CrossRef\]](#)
- Witte, D.; Gallian, J.A. A survey: Hamiltonian cycles in Cayley graphs. *Discret. Math.* **1984**, *51*, 293–304. [\[CrossRef\]](#)
- Riyas, A.; Geetha, K. A study on Cayley graphs over dihedral groups. *Int. J. Math. Comb.* **2017**, *1*, 63–70.
- Tripi, A. Cayley Graphs and Their Applications. Master's Thesis, Missouri State University, Springfield, MO, USA, 2017.
- Lu, L.; Mönius, K. Algebraic degree of Cayley graphs over abelian groups and dihedral groups. *J. Algebr. Comb.* **2023**, *57*, 753–761. [\[CrossRef\]](#)
- Babai, L. Spectra of Cayley graphs. *J. Comb. Theory* **1979**, *27*, 180–189. [\[CrossRef\]](#)
- Sarmin, N.H.; Fadzil, A.F.A.; Erfanian, A. Seidel energy for Cayley graphs associated to dihedral groups. *J. Phys. Conf. Ser.* **2021**, *1988*, 012066. [\[CrossRef\]](#)
- Peyerimhoff, N.; Vdovina, A. Cayley graph expanders and groups of finite width. *J. Pure Appl. Algebra* **2011**, *215*, 2780–2788. [\[CrossRef\]](#)
- Charles, D.X.; Lauter, K.E. Cryptographic hash functions from expander graphs. *J. Cryptol.* **2009**, *22*, 93–113. [\[CrossRef\]](#)
- Jao, D.; Miller, S.D. Expander graphs based on GRH with an application to elliptic curve cryptography. *J. Number Theory* **2009**, *129*, 1491–1504. [\[CrossRef\]](#)
- Sosnovski, B. Cayley Graph of Semigroups and Applications to Hashing. Doctoral Dissertation, City University of New York, New York, NY, USA, 2016.
- Chen, P. A kind of graph structure of rings. *Algebra Colloq.* **2003**, *10*, 229–238.
- Green, E.L.; Schroll, S. Brauer configuration algebras: A generalization of Brauer graph algebras. *Bull. Sci. Math.* **2017**, *121*, 539–572. [\[CrossRef\]](#)
- Schroll, S. Brauer Graph Algebras. In *Homological Methods, Representation Theory, and Cluster Algebras, CRM Short Courses*; Assem, I., Trepode, S., Eds.; Springer: Cham, Switzerland, 2018; pp. 177–223.
- Espinosa, P.F.F. Categorification of Some Integer Sequences and Its Applications. Doctoral Dissertation, National University of Colombia, Bogotá, Colombia, 2021.
- Cañadas, A.M.; Gaviria, I.D.M.; Vega, J.D.C. Relationships between the Chicken McNugget Problem, Mutations of Brauer Configuration Algebras and the Advanced Encryption Standard. *Mathematics* **2021**, *9*, 1937. [\[CrossRef\]](#)

22. Cañadas, A.M.; Ballester-Bolinches, A.; Gaviria, I.D.M. Solutions of the Yang-Baxter equation arising from Brauer configuration algebras. *Computation* **2022**, *11*, 1–17. [[CrossRef](#)]
23. Cañadas, A.M.; Rios, G.B.; Serna, R.-J. Snake graphs arising from groves with an application in coding theory. *Computation* **2022**, *10*, 1–17. [[CrossRef](#)]
24. Cañadas, A.M.; Angarita, M.A.O. Brauer configuration algebras for multimedia based cryptography and security applications. *Multimed. Tools. Appl.* **2021**, *80*, 23485–23510.
25. Agudelo, N.; Cañadas, A.M.; Gaviria, I.D.M.; Espinosa, P.F.F. $\{0, 1\}$ -Brauer configuration algebras and their applications in the graph energy theory. *Mathematics* **2021**, *9*, 3042. [[CrossRef](#)]
26. Pan, J.W.; Chen, Z.B.; Lu, C.Y.; Weinfurter, H.; Zeilinger, A.; Żukowski, M. Multiphoton entanglement and interferometry. *Rev. Mod. Phys.* **2012**, *84*, 777–838. [[CrossRef](#)]
27. The Nobel Prize in Physics 2022. NobelPrize.org. Nobel Prize Outreach AB 2024. Available online: <https://www.nobelprize.org/prizes/physics/2022/summary/> (accessed on 1 February 2024).
28. Krenn, M.; Gu, X.; Zeilinger, A. Quantum experiments and graphs I: Multipartite states as coherent superpositions of perfect matchings. *Phys. Rev. Lett.* **2017**, *119*, 240403. [[CrossRef](#)]
29. Gu, X.; Erhard, M.; Zeilinger, A.; Krenn, M. Quantum experiments and graphs II: Quantum interference, computation, and state generation. *Proc. Natl. Acad. Sci. USA* **2019**, *116*, 4147–4155. [[CrossRef](#)]
30. Gu, X.; Chen, L.; Zeilinger, A.; Krenn, M. Quantum experiments and graphs. III. high-dimensional and multiparticle entanglement. *Phys. Rev. A* **2019**, *99*, 032338. [[CrossRef](#)]
31. Rankin, R.A. A campanological problem in group theory. *Proc. Camb. Philos. Soc.* **1948**, *44*, 17–25. [[CrossRef](#)]
32. Brian, A.; Chen, C.C.; Mathew, D. Hamiltonian paths in Cayley graphs on generalized dihedral groups. *Filomat* **2019**, *33*, 3599–3613.
33. Pastine, A.; Jaume, D. On Hamiltonian circuits in Cayley digraphs over generalized dihedral groups. *Rev. Unión Matemática Argent* **2012**, *53*, 79–87.
34. Palanivel, N.; Chithra, A.V. Energy and Laplacian energy of unitary addition Cayley graphs. *Filomat* **2019**, *33*, 3599–3613. [[CrossRef](#)]
35. Brualdi, R.A. *Introductory Combinatorics*; Pearson and Prentice Hall: Old Bridge, NJ, USA, 2010.
36. Diestel, R. *Graph Theory*, Electronic ed.; Springer: New York, NY, USA, 2000.
37. Kühn, D.; Osthus, D. A survey on Hamilton cycles in directed graphs. *Eur. J. Comb.* **2012**, *33*, 750–766. [[CrossRef](#)]
38. Darbinyan, S.K. On Hamiltonian and Hamilton-connected digraphs. *arXiv* **2018**, arXiv:1801.05166v1.
39. Nash-Williams, C.S.J.A. Hamilton circuits in graphs and digraphs. In *The Many Facets of Graph Theory*; Springer: Berlin/Heidelberg, Germany, 1968; Volume 110, pp. 237–243.
40. Andrews, G.E. *The Theory of Partitions*; Cambridge University Press: Cambridge, UK, 2010.
41. Sierra, A. The dimension of the center of a Brauer configuration algebra. *J. Algebra* **2018**, *510*, 289–318. [[CrossRef](#)]
42. Schibell, S.T.; Stafford, R.M. Processor interconnection networks from Cayley graphs. *Cryptol. Q.* **2011**, *3929129*, 35–55. [[CrossRef](#)]
43. IBM. What Is Quantum Cryptography? Available online: <https://www.ibm.com/topics/quantum-cryptography> (accessed on 15 November 2023).
44. Jacques, S.; Naehrig, M.; Roetteler, M.; Virdia, F. Implementing Grover Oracles for Quantum Key Search on AES and LowMC. In Proceedings of the 39th Annual International Conference on the Theory and Applications of Cryptographic Techniques, Advances in Cryptology, EUROCRYPT 2020, Zagreb, Croatia, 10–14 May 2020; Canteaut, A., Ishai, Y., Eds.; Lecture Notes in Computer Science; Springer: Cham, Switzerland, 2020; Volume 12106.
45. Yin, J.; Li, Y.H.; Liao, S.K.; Yang, M.; Cao, Y.; Zhang, L.; Ren, J.G.; Cai, W.Q.; Liu, W.Y.; Li, S.L.; et al. Entanglement-based secure quantum cryptography over 1,120 kilometres. *Nature* **2020**, *582*, 501–505. [[CrossRef](#)] [[PubMed](#)]
46. Sloane, N.J.A. On-Line Encyclopedia of Integer Sequences. Available online: <http://oeis.org/A001045> (accessed on 20 October 2023).

Disclaimer/Publisher’s Note: The statements, opinions and data contained in all publications are solely those of the individual author(s) and contributor(s) and not of MDPI and/or the editor(s). MDPI and/or the editor(s) disclaim responsibility for any injury to people or property resulting from any ideas, methods, instructions or products referred to in the content.